Experimental testing of Coorong filamentous algal growth with increasing temperature and salinity

Michelle Waycott, Andrew McDougall, Emma O'Loughlin

Goyder Institute for Water Research

Technical Report Series No. 19/36

www.goyderinstitute.org

Goyder Institute for Water Research Technical Report Series ISSN: 1839-2725

The Goyder Institute for Water Research is a partnership between the South Australian Government through the Department for Environment and Water, CSIRO, Flinders University, the University of Adelaide, the University of South Australia and the International Centre of Excellence in Water Resource Management. The Institute enhances the South Australian Government's capacity to develop and deliver science-based policy solutions in water management. It brings together the best scientists and researchers across Australia to provide expert and independent scientific advice to inform good government water policy and identify future threats and opportunities to water security.

This program is part of the Department for Environment and Water's Healthy Coorong Healthy Basin Program, which is jointly funded by the Australian and South Australian governments.

Enquires should be addressed to: Goyder Institute for Water Research
Level 4, 33 King William Street
Adelaide, SA 5000
tel: 08 8236 5200
e-mail: enquiries@goyderinstitute.org

Citation

Waycott, M., McDougall, A., and O'Loughlin, E. (2019) *Experimental testing of Coorong filamentous algal growth with increasing temperature and salinity.* Goyder Institute for Water Research Technical Report Series No. 19/36.

Disclaimer

Contents

Figures

Tables

Executive summary

Filamentous green algal blooms have been forming annually in the Coorong, South Australia, and have been documented to occur over many locations and large areas (many hectares) since 2010. It is believed that as low salinity and elevated water levels were returned to the Coorong after a decade of drought, filamentous algal growth was favoured leading to smothering of the keystone seagrass species *Ruppia tuberosa*. Management options to reduce the impact of the algal blooms on the Coorong ecosystem requires information on their sensitivity to changes in the environment. Experimental studies have recently been completed (Collier et al. 2017) confirming a salinity threshold for algal growth in the southern Coorong of 90 ppt. However, the experimental testing of algal survival thresholds was conducted at a moderate temperature (~20°C). As algal growth rates vary dramatically the temperature responses of algal growth were required to be tested to determine the relationship between water temperature and algal growth.

The utility of this growth rate data is to support the improvement of a biogeochemical-hydrological model that enables testing of the system scale changes that are expected to occur under different environmental and management scenarios. Filamentous algal growth impacts the ability of the aquatic plant *Ruppia tuberosa* to establish, thrive and reproduce during the limited growing season of the southern Coorong. The observation of larger areas of algal growth also indicate a shift in the overall community composition of primary producers across the whole Coorong ecosystem.

The growth rates of the filamentous green algal community that currently dominates aquatic plant productivity in the central and southern Coorong are controlled by the combination of salinity and temperature under conditions of excess nutrients. We undertook an aquatic plant culture based experimental approach to test filamentous algal survival thresholds for the previously identified *Ulva paradoxa* filamentous green algal community present in the area. The algal bloom formation is at its maximum during the late spring-early summer period. To determine equivalent *in situ* temperature data we deployed temperature loggers in three locations in the central, mid-southern and southern areas of the Coorong southern lagoon.

The experimental testing identified that for salinities from 35—90 ppt, an optimum temperature for the *Ulva paradoxa* filamentous green algal community was 30°C, that is the temperature where the relationship between weight gain is the most positive. Salinities of more than 90 ppt were the most significant at reducing filamentous green algal growth rates. At lower salinities the algae appear resilient to a wide range of temperatures and from previous studies, nutrient availability.

Overall the following outcomes were observed: for all salinity data, as salinity increases, weight change decreases as a negative linear relationship; for temperature > 30°C there is a positive linear relationship with weight change; for temperatures ≤30°C there is a negative linear relationship.

Modelling of filamentous algal growth responses enabled the definition of relationships between algal net weight gain, salinity and temperature with the following formulae:

For temperatures 20—30°C:

The weight change (mg) = 139.671 – 4.433 (salinity ppt) + 12.087 (temperature °C)

For temperatures 30—35°C:

The weight change (mg) = 838.999 – 5.283 (salinity ppt) – 8.98 (temperature °C)

These relationships can be applied in the hydrodynamic-biogeochemical model of the Coorong developed by Hipsey et al. (2016) and presented with more detail in Collier et al. (2017). The ability to utilise this model to predict the impact of variable inter-annual seasonal conditions or different scenarios for the use of environmental water will improve options for the management of the Coorong. In addition, these data will contribute to establishing options to enable further restoration of *Ruppia* in the Coorong by identifying preferred habitat suitability, which is currently limited substantially by filamentous algal growth.

Acknowledgments

This program is part of the Department for Environment and Water's Healthy Coorong Healthy Basin (HCHB) Program, which is jointly funded by the Australian and South Australian governments. We wish to acknowledge support from Dr Catherine Collier, TropWater, James Cook University for use of the Diving PAM for these experiments as well as ongoing discussion and advice on the experimental treatments. We thank the HCHB team, particularly Jody O'Connor, Bec Quin, Matt Gibbs and for contributions made by other HCHB leadership team members for discussion leading to improving the scope of this work. We thank Nicole Foster for supporting additional field work and assisting with experiments. We thank Rob Reid from The University of Adelaide, School of Biological Sciences for supporting development of the experimental setup at the University of Adelaide and the Faculty of Sciences staff, Sean Connell and other users of the Aquatic Growth facilities in allowing establishment of the new growth setup in the Benham Laboratories. We thank David Paton and his team for their ongoing willingness to share data and to work to improve the health of the Coorong. We would also like to thank Geoff Gallasch, President of the Coorong Shack Owners Association for valuable discussions and insight into the changing nature of the Coorong waters and assisting us with understanding the dynamics of the filamentous algal blooms.

1 Introduction

The seagrass *Ruppia tuberosa* is a keystone species of the aquatic plant community across the shallower benthic habitat of the Coorong, South Australia (Womersley 1975). The Coorong and Lakes Alexandrina and Albert in South Australia was designated as a Wetland of International Importance under the Ramsar Convention in 1985, in recognition of its role in supporting a wide range of habitat types and vast numbers (hundreds of thousands) of waterbirds (Paton et al. 2009, Paton 2010) many that forage on *R. tuberosa*.

Seagrass meadows are particularly vulnerable to algal blooms because they have overlapping ecological niches and seagrasses can act as a substrate for bloom formation (Tweedley et al. 2008). Competition occurs between algae and seagrass for space, nutrients and light (Figure 1), and as the algae blooms their biomass will intercept sunlight, reducing photosynthetic rates of seagrass (Coffaro and Sfriso 1997, Cummins et al. 2004, Han et al. 2016). As a result of light limitation, seagrass growth rates and density decline, leading to contraction of the seagrass colonisation depth (Han and Liu 2014) and overall biomass in the ecosystem. Small statured seagrass species such as *Ruppia* are particularly vulnerable to the impacts of bloom formation due to their limited energy stores (Holmer and Nielsen 2007), reducing the time they can persist under low light conditions.

Once established, algal blooms decay and the resulting decomposition processes consumes oxygen in the sediment, leading to sediment anoxia (McGlathery et al. 2007). Bloom decay and sediment anoxia can have dramatic effects, including higher turnover rates of organic nutrients, loss of stabilising primary producers such as seagrasses, lost of benthic invertebrate communities and an increased production of ammonium leading to destabilised benthic food webs (Osterling and Pihl 2001, Cummins et al. 2004).

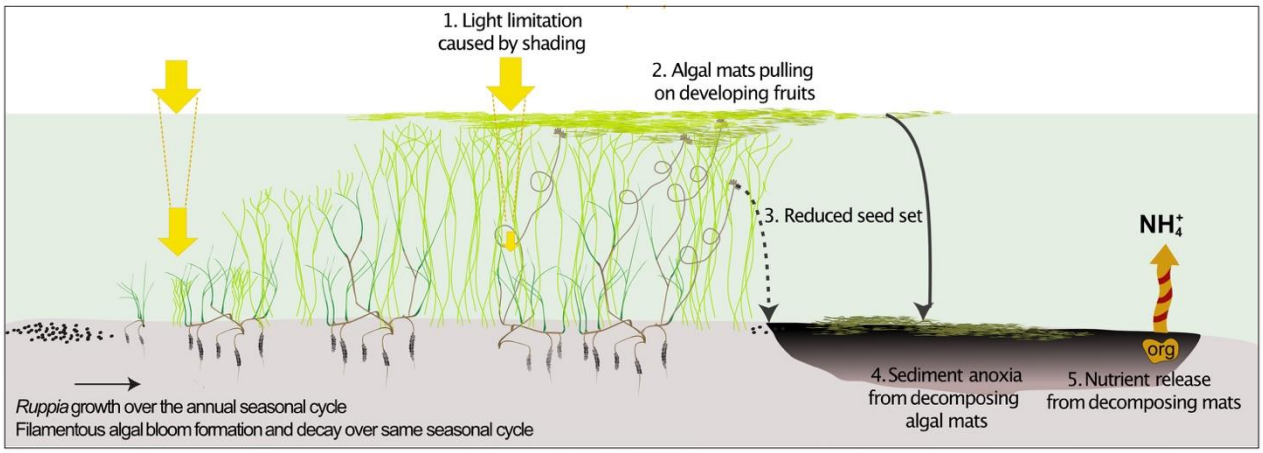

Figure 1. Conceptual diagram depicting development of *Ruppia tuberosa* communities over the growing season (summer seed bank through autumn germination, winter and spring growth and initiation of flowering to summer seed set and consequences of algal blooms) and the formation and decay of algal blooms highlighting observed impacts of the blooms on *R. tuberosa* (modified from Collier et al. 2017).

Seasonal blooms of the filamentous green algae community comprising *Ulva paradoxa*, *Cladophora* sp. and *Rhizoclonium* sp. have been observed (Paton et al. 2011, Frahn et al. 2012, Collier et al. 2017). These blooms were detected across 11 of 14 widely dispersed sites across the southern lagoon in December 2011 when water levels were returned to the Coorong following the extended period of drought referred to as the 'millennium drought' (Paton et al. 2011). The density and location of the blooms has been variable from 2011 to 2015 (Frahn and Gehrig 2015) but in 2016, there were widespread rafts of blooms forming to the north and the south of Parnka Point (Paton et al. 2017; Collier et al. 2017). These blooms have been observed to directly interfere with reproductive outputs of *R. tuberosa* and *Althenia cylindrocarpa* (synonymous name for *Lepilaena cylindrocarpa*) (Paton et al. 2011, Collier et al. 2017) and as a result will be affecting the ecological services that contribute to the site's international significance.

Despite occurring naturally in regional estuarine environments (Collier et al. 2017), these filamentous green algae are rapidly-growing opportunistic species that have a high demand for nitrogen (Lavery and McComb 1991, Pedersen and Borum 1996). Indeed, nitrogen was found to be the primary limiting factor *in situ* in the Coorong (Collier et al. 2017) and under experimental conditions to test plant responses to salinity. Filamentous algal blooms dominated by *Ulva* are dependent on a constant high supply of nutrients (Coffaro and Sfriso 1997) and nutrient reduction is a primary management option for preventing bloom formation. It is plausible, under very high nutrient loads that phosphorus may become limiting. The filamentous algal blooms are symptomatic of excessive system-scale nutrient loads or even eutrophic ecosystems and are sometimes referred to as nuisance algae (Nelson et al. 2015). In addition, the extreme hypersalinity experienced in the southern Coorong during the growing period means few comparative data are available for predicting growth responses to varying conditions (summarised in Collier et al. 2017).

The development of a Habitat Suitability Index (HSI) by Collier et al. (2017) for *Ruppia* in the Coorong includes the parameterisation of filamentous algal growth rates and distribution as a modifier of *Ruppia* survival by Collier et al. (2017) who identified analytically the critical role that the filamentous algae play in seagrass community development. Evaluating annual timing is important because it appears that the blooms are coincident with inhibition of *Ruppia* flowering and seed set (Paton et al. 2017, Collier et al. 2017). The annual timing of filamentous algal blooms on the scale observed in the southern Coorong in the past 9 years is associated with particular environmental conditions. These conditions include; southern Coorong water levels, light availability, salinity, nutrients and temperature. Previous experimental research identified salinity thresholds of 70-90 ppt above which filamentous algal growth stopped or where algae died under higher nutrient conditions (Collier et al. 2017). Growth rates were also observed to decline under conditions of low salinity and nutrient levels. In all of these experiments, growth responses were tested under constant conditions of approximately 22°C and constant light availability. Seasonal growth of algae will increase with warming water temperatures, thus, to inform the Habitat Suitability Index, model parameterisation of temperature is required.

The objectives of this study were to assess how the bloom forming filamentous green algal community of the Coorong respond to changes in temperature under a range of salinities with elevated nutrient loads. The results of this assessment will be used to generate an updated model to predict habitat suitability for *Ruppia tuberosa* growth in the Coorong as described by Collier et al. (2017).

2 Methods

2.1 Materials

Filamentous green algae that are associated the benthic plants of the southern Coorong were collected from the waters surface at Salt Creek, The Coorong, South Australia (36°07'12.7"S 139°38'12.0"E; Figure 2) and transported in site water to the aquatic growth rooms of The University of Adelaide's Benham Laboratories. Verification of the algal species present was conducted by visual identification of staff at the State Herbarium of South Australia, where vouchers of the original source material have been lodged for incorporation into the permanent collection. Species identification confirmed that the filamentous algal community was consistent with those identified in algal blooms by Collier et al. (2017), an extension of the combined model described in Hipsey et al. (2016). The algae were a mixed community dominated by *Ulva paradoxa* with cooccurring species *Cladophora* sp. and *Rhizoclonium* sp. and identified using The Marine Benthic Flora of South Australia and Algae Net (Collier et al. 2017).

2.2 Experimental setup

Within the aquatic growth rooms at the University of Adelaide Benham Laboratories aquatic growth rooms algal growth experimental units were established and the field harvested algae were placed in aerated plastic containers with a culture medium that included; natural seawater (38 g/L NaCl), calcium carbonate chips to regulate pH and f/2 equivalent (Varicon Aqua Cell-hi F2P powder) to an estimated final concentration of 8.82 mM NO_3^{-1} and 0.362 mM PO_4^{3-} for experimentation based on manufacturer data. Nutrient concentrations for experimentation were based on experimental outcomes from analysis of salinity and nutrient interactions presented in Collier et al. (2017). All experiments were conducted in this same culture medium, only modified by changing salinity through the addition of commercial grade NaCl to increase salinity or spring water to decrease salinity to the final experimental concentration. The culture and the experimental units were grown under Phillips GreenPower LED lights (Phiillips™ product number: GP LED DR/W 150LB, a light source optimised for closed, climate-controlled cultivation facilities) at a day to night ratio of 15:9. This provided estimated light output equivalent to approximately 400 µmol m^{-2} s^{-1}, which equates to providing greater than light saturation conditions (E_k) for filamentous *Ulva linza* (i.e. approximately 90 – 250 □mol photons m^{-2} s^{-1}) (Kim et al. 2011). Culture stocks were maintained at 22°C during the day and 18°C at night. A water change occurred once a week and the algae were acclimated to these lab conditions for at least two months prior to experimentation. Culture growth monitoring prior to experimentation included salinity (measured with a Milwaukee MA887 Digital Seawater Refractometer) temperature (measured with a DeltaTrak 11040) and (pH measured with an EZDO pH7200).

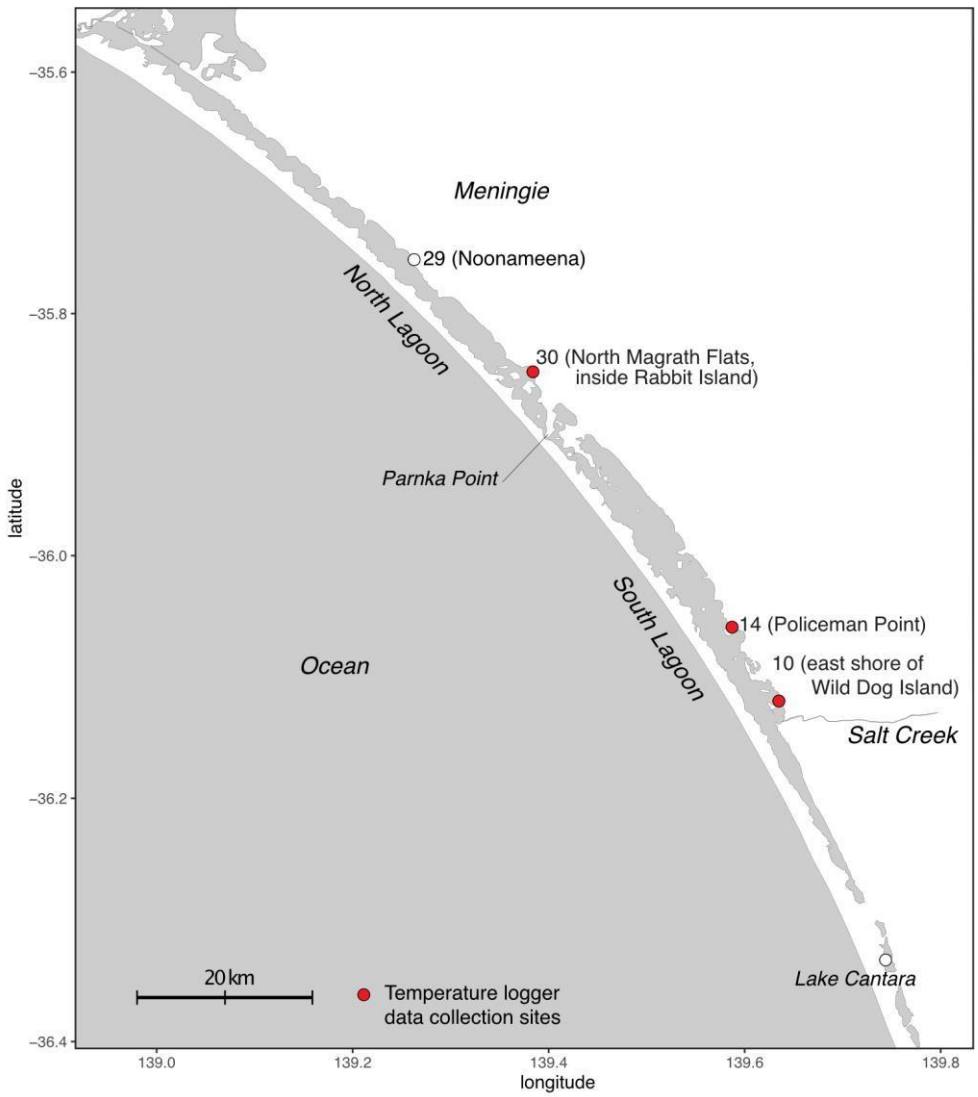

Figure 2. Location of collections of algal source material (Salt Creek) and shallow water temperature logger deployment associated with existing *in situ* structures. Site numbers refer to those published in Collier et al. (2017) for reference.

The experimental setup (Figure 3a) included four (4) replicate tanks comprised of plastic 32 L bins each with independent water temperature moderation and a light source. In each bin were five, identical 1.7 L glass containers hereafter referred to as mini-cosms, which were provided with continuous aeration (Figure 3b). Each glass container was assigned a location number and a randomised allocation of salinity treatment (Figure 3a). Temperature was controlled using in-tank thermoregulators, and monitored using an in-tank temperature logger. To maintain even thermoregulation, an insulating layer made from a foamed polymer blend of PVC and nitrile rubber, was wrapped around the outside of the replicate tanks to minimise tank temperature variation from external sources.

a)

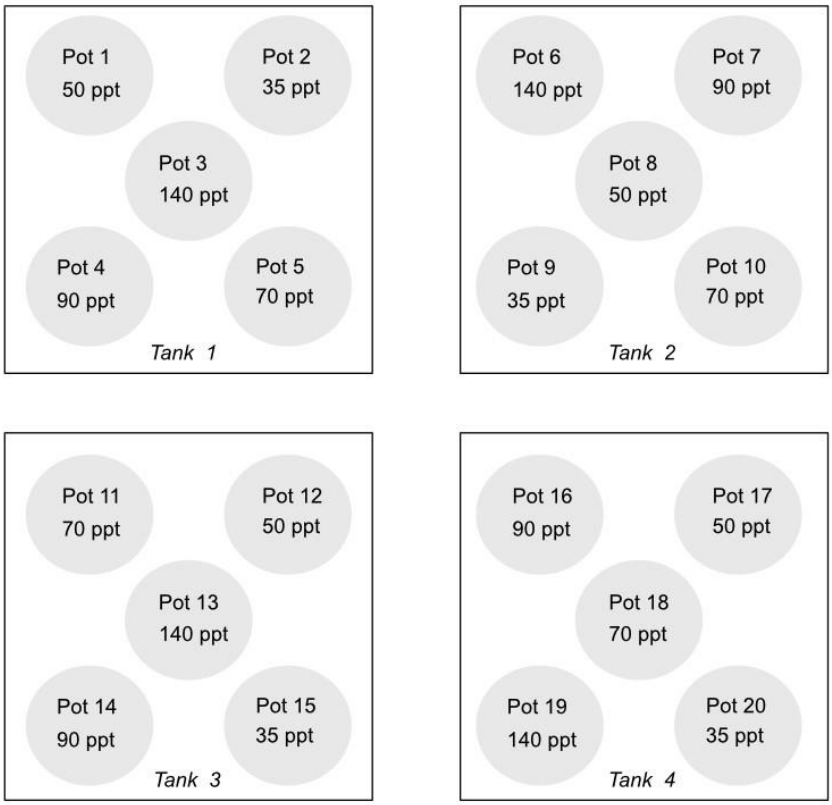

b)

Figure 3. a) Schematic of experimental layout demonstrating the relative positions of each tank and mini-cosm unit (i.e. pots) assigned salinity treatment. b) Photograph of two (2) replicates of the experimental units, mini-cosm salinity treatments during establishment of each experimental trial with insulating layer removed to visualise the tanks (photograph by Emma O'Loughlin).

TREATMENTS

Experiments were conducted as a series of independent temperature experiments with controlled replicates for different salinities. We chose five (5) different salinities to represent the critical range established in Collier et al. (2017) for algal growth limitation or mortality: 35, 50, 70, 90, 140 ppt (parts per thousand). These reflect a range from below marine salinity (35 ppt) to extreme hypersalinity (140 ppt). Previous experiments demonstrated that at growing conditions of 22°C algal mortality occurred at above 90 ppt and limited growth occurred at 60 ppt (Collier et al. 2017). Temperature treatments were run separately as short-time period response experiments, each temperature independently run for 5 days as described in the experimental setup matrix (Table 1). Different temperature treatments were each run independently for 5 days to deliver the final experimental setup (Table 1).

Table 1. Experimental treatments for testing temperature responses of filamentous green algae sourced from the Coorong (southern Lagoon) to a range of salinities for change in net growth and effective quantum yield.

Experiment replicate	Experimental target temperature	Temperature range logged over course of the experiment	Salinity treatments	Number of replicate tanks
1	20°C	20.12-22.18°C	35, 50, 70, 90, 140 ppt	4
2	25°C	20.2-26.04°C	35, 50, 70, 90, 140 ppt	4
3	30°C	28.4-30.46°C	35, 50, 70, 90, 140 ppt	4
4	35°C	32.52-36.93°C	35, 50, 70, 90, 140 ppt	4

Algal culture handling methods were standardised to those utilised in Collier et al. (2017). At the start of each experiment, algae were collected from the stock culture, patted dry to remove excess water until a colour change from dark green to light green was observed, weighed (starting weight in milligrams) and placed in containers arranged in a random order relative to each other spatially (Figure 3a). On each day, at the same time of day in the light cycle, the effective quantum yield of photosystem II ($ø_{PSII}$), a measure of the amount of photosynthesis by the plants (algae), was measured on two separate segments of algae within each container on algal material that had not been dark adapted prior to measurement. Effective quantum yield, measured using a Diving PAM fluorometer (WALZ GmBH) using the following settings (MI=8; SI=8; G=2), indicates the efficiency that the photosynthetic apparatus can convert sunlight into chemical energy for carbon fixation, and ultimately growth. Effective quantum yield was calculated according to the following formula:

a. $ø_{PSII} = (F'_m - F)/F'_m$

where F'_m is the maximum light-adapted fluorescence yield and F is the minimum light-adapted fluorescence yield.

At the end of the experiment samples were re-weighed in the same manner as at the beginning (final weight, mg). The final result was estimated as the net change in weight (mg) from day 0 to day 4 (i.e. weight gained or lost) and the final effective quantum yield ($ø_{PSII}$).

2.3 Field based temperature data

To evaluate field-based temperature ranges HOBO Pendant MX Water Temperature Loggers (HOBO MX2201) were deployed in shallow water typical of where algal blooms form at three locations (Figure 2). Loggers were set to record data every 15 minutes and were initially deployed for approximately 2 months at water depths which varied from 0.3 m—0.8 m at time of deployment (3 and 4 October 2019). Loggers were collected and data downloaded for analysis and additional loggers were deployed as replacements to continue collecting

data. Each data point was plotted to visualise the range of temperatures over the day and across the period of monitoring.

2.4 Statistical analysis

Preliminary analysis of the results was conducted using statistic software SPSS with outcomes of experiments measured as net weight of algal growth (mg) and effective quantum yield ($ø_{PSII}$). Statistical modeling to evaluate the relationship between temperature and algal growth under different salinity treatments was then implemented using the "haven" package and data files were read into rStudio to create r data frames (Muggeo et al. 2008). This has the advantage that data files may be stored and read without opening the statistical software program, thus enabling more rapid data checking and exploration. Initial plots were created to visualise and inspect the data. Using an assumption that weight change over the experiment period was an indicator of biological activity, only positive weight changes were taken to be data from living organisms, and negative weight changes were assumed to be due to the death of the organism at some time during the experiment. To test the effects of increasing salinity on weight change as a function of temperature, the combined experimental data was used to model the potential for a 'break point' in how plants responded under different temperatures. This was done by comparing net weight change associated with salinity at all temperatures and determining if the modelled relationships (visualised as loess plots) could be described by more than one linear relationship.

It should be noted that the 'break point' is the point at which the slope of the line changes in the modelled output based on experimental data (e.g. Appendix Figure A3). For the weight change x temperature relationship, the break point should only be considered from the positive weight change data, since it is assumed to be a biological response, and the negative weight change data is assumed to be associated with dead or dying plant material. For estimation of this break point, it is appropriate with these data to read directly off the loess plots (Appendix A), since there are only four discrete temperatures at which the experiment was conducted. This break point is approximately 30°C.

A negative relationship, for the interaction by weight change x temperature it was assumed to be the result of growing living organisms as long as the weight change is greater than 0 in these analyses.

A more precise estimation of this break point was produced with the r package "segmented" (Wickham and Miller 2019; Appendix A).

These models were run to determine relationships in the following ways:

- For all salinity data, determine if as salinity increases, weight change decreases as a negative linear relationship.
- For temperature > 30°C determine if there is a positive linear relationship with weight change.
- For temperatures <=30°C determine if there is a negative linear relationship.

The interaction between salinity and temperature were also evaluated for significance. Models, visualised as loess plots, were generated for all temperatures and determined if they had a significant interaction with salinity (Appendix A). These models were used to determine if there are different relationships between weight change and salinity as temperature increases, and assessing if it is appropriate to fit more than one model for algal growth responses to temperature.

3 Results

3.1 Temperature responses with varying salinity

A significant relationship between temperature and salinity was determined for filamentous algal growth in culture for algal net weight change over the course of the experiments and the effective quantum yield (Appendix A). Statistical analysis indicated greatest increase in weight at 30°C (Figure 4) and at the lowest salinity (Figure 5). Filamentous algal growth declined (net weight zero or negative) at all temperatures (Figure 4) but algal death (loss of net weight) was only observed for the higher salinities (Figure 5). The reduction in photosynthetic capacity measured as effective quantum yield was most pronounced at higher salinities (Figure 6–7). These analyses confirm that salinity provides the greatest driver of filamentous algal growth rate reduction however there is a rate response associated with temperature.

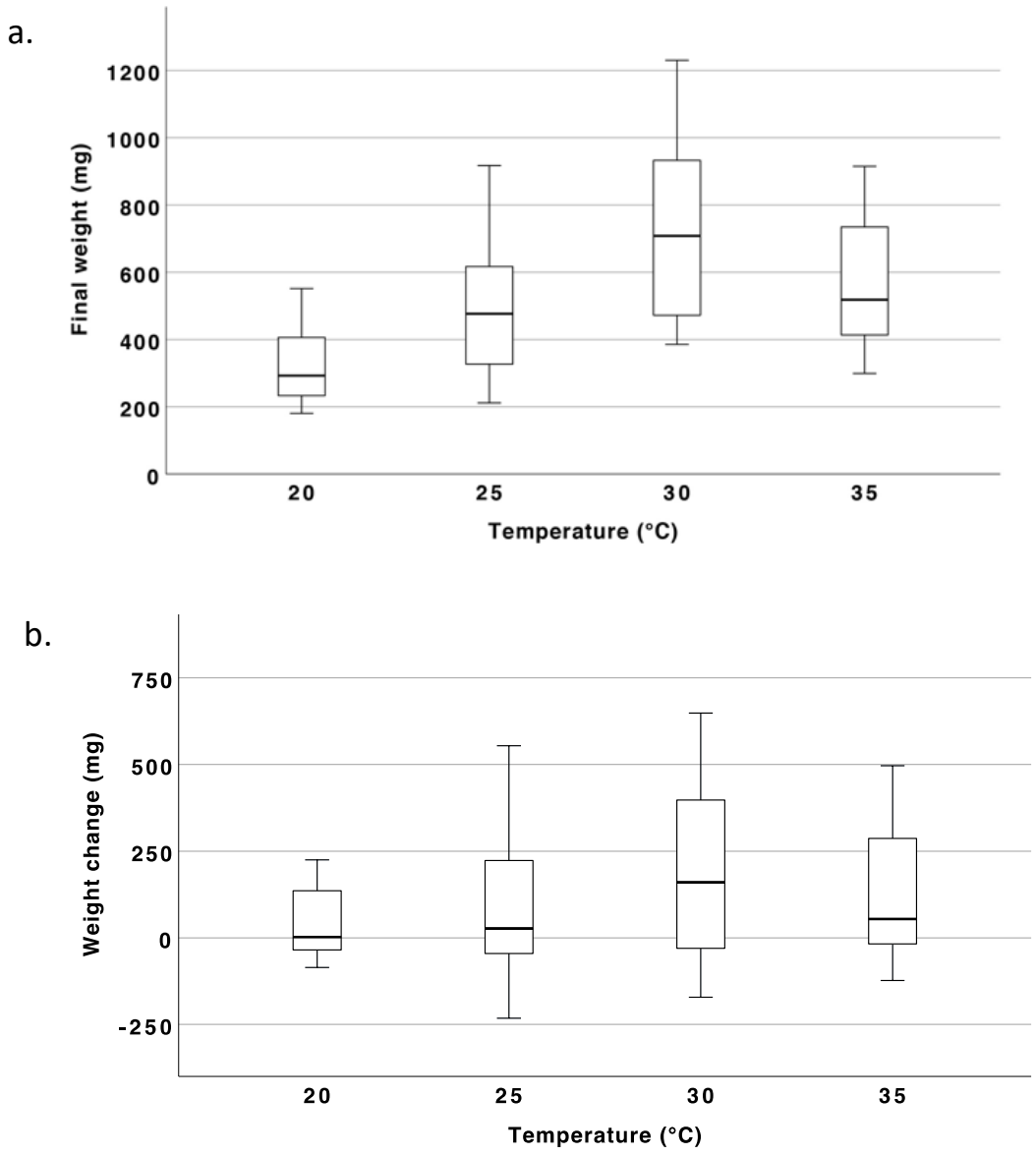

Figure 4. Experimental weights (mg) at end of 5 day treatments for all salinities grouped at each temperature presented as box plots. a. Final experimental weight (mg). b. Net weight change (mg) over the 5 day experiment.

a.

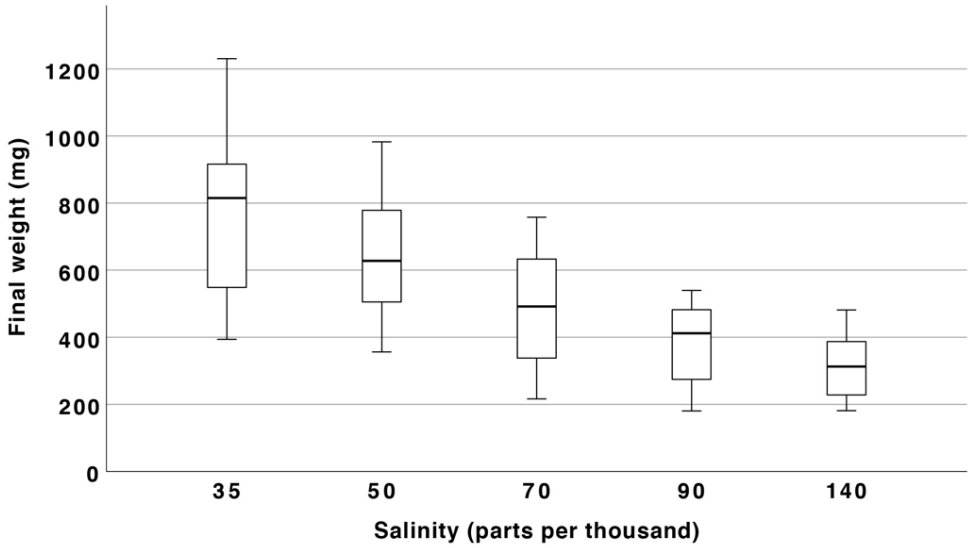

b.

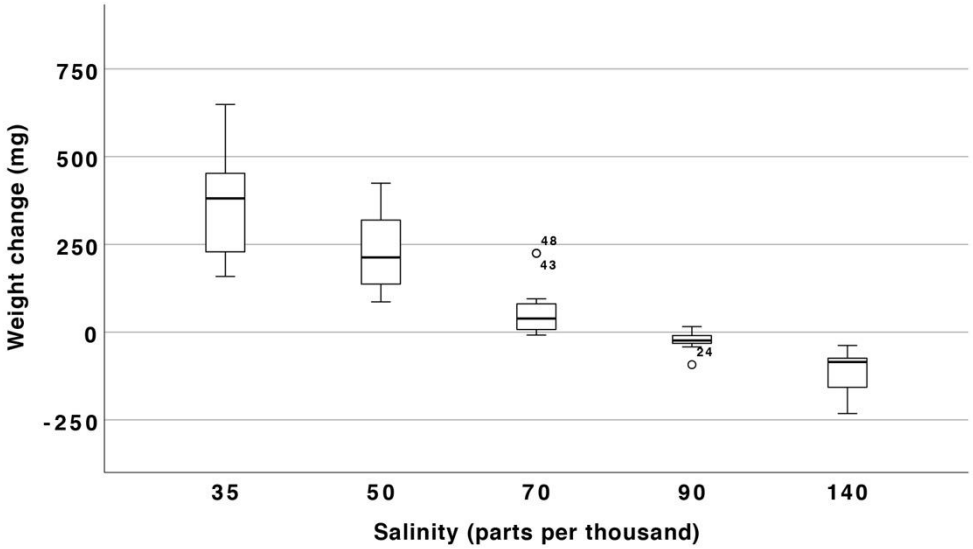

Figure 5. Experimental weights (mg) at end of 5 day treatments for all temperatures grouped at each salinity presented as box plots. a. Gross final weight total (mg). b. Net weight change (mg) over the 5 day experiment.

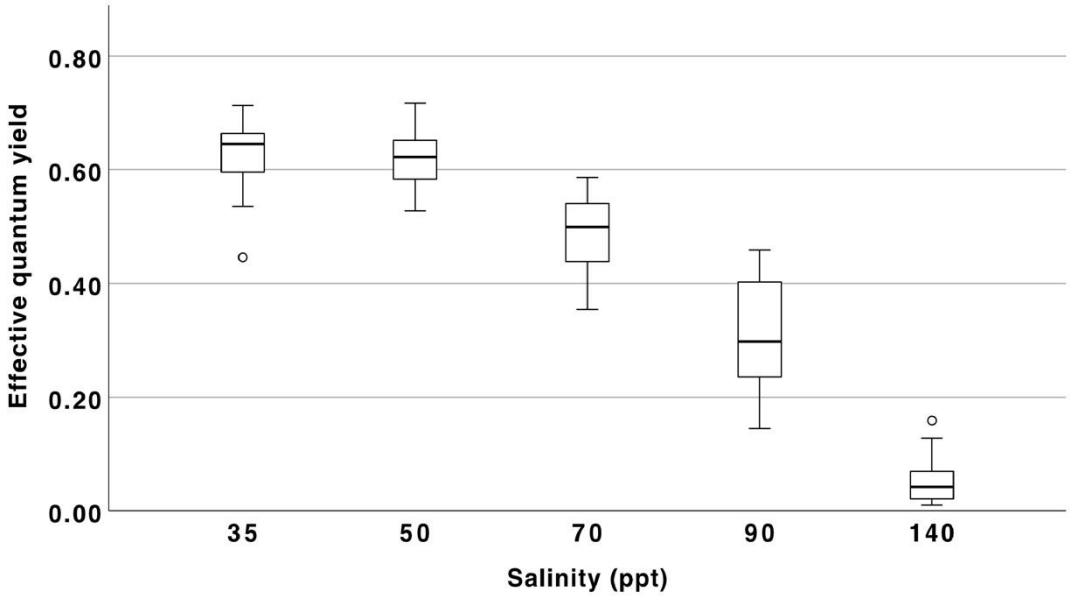

Figure 6. Box plots of the response to salinity as a measure of plant oxygen production and an indicator of relative plant performance at the end of 5 day treatments for filamentous green algae grown in culture with results from all temperatures grouped at each salinity presented as box plots.

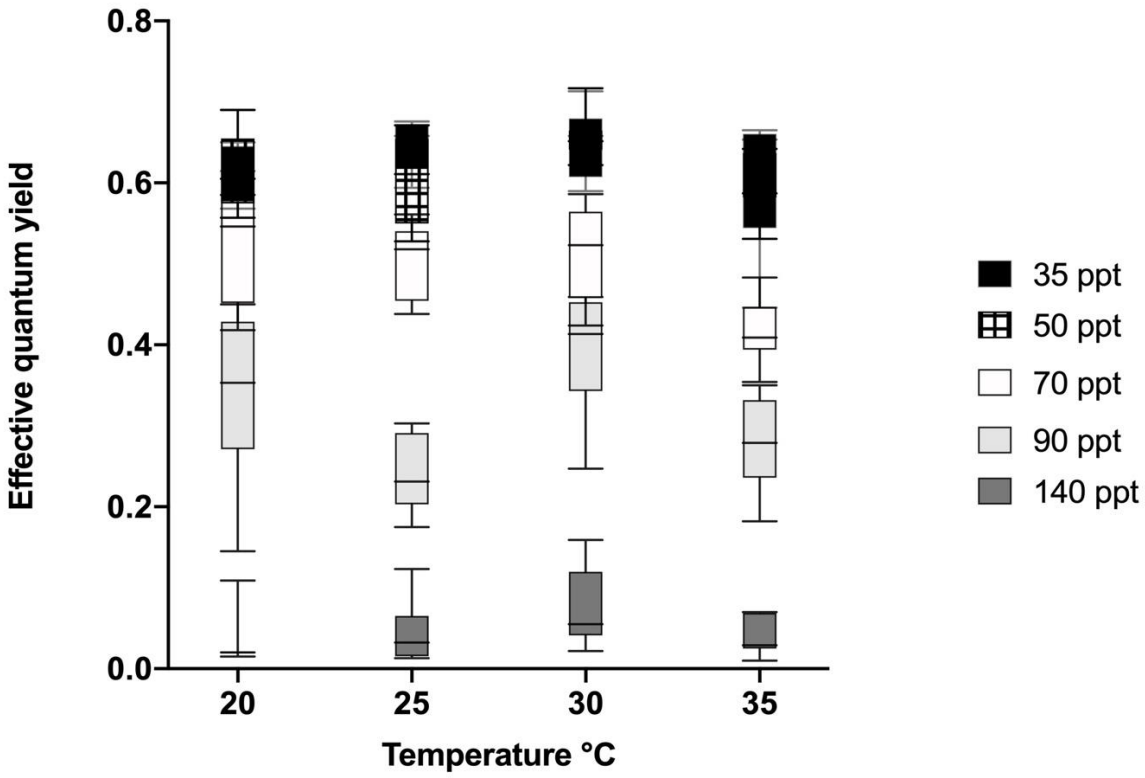

Figure 7. Box plots of the response to temperature as a measure of plant oxygen production and an indicator of relative plant performance at the end of 5 day treatments for filamentous green algae grown in culture for all salinities at each temperature.

Based on the analysis of the total data set, two linear predictive models for weight change were resolved; one for experimental results for treatments up to and including 30°C and another for 30°C and over. The negative impact of treatment on filamentous algae was taken to be where the weight change is equal to zero, and this value was used to model possible thresholds for algal growth evident from these data (Tables 2—5). This was done because there were significant interactions between the temperatures at which the observations were made and salinity (Appendix A) and there was a non-linear effect in the data, but either side of the turning point, there are strong linear relationships (Appendix A). Fitting a generalised additive model was not possible because a term (temperature) has fewer unique covariate combinations than specified maximum degrees of freedom, since temperature readings were made at 20, 25, 30, and 35°C only. In addition, two linear models and a set of tables of predictions have been calculated for the modelled mean quantum yield for temperature and salinity, and these follow the method for the weight change models.

The model outcomes were derived as formulas that were experimentally determined by the statistical analysis:

- For temperatures 20—30°C:

  The weight change (mg) = 139.671 – 4.433(salinity ppt) + 12.087(temperature °C)

- For temperatures 30—35°C:

  The weight change (mg) = 838.999 – 5.283(salinity ppt) – 8.98(temperature °C)

These formulas were then used to determine the different predicted scenarios which result in weight change = 0, and the results given in Tables 2–5. It must be noted that only predictions made from within the range of experimental variables can be considered.

In addition, two linear models were developed for effective quantum yield x temperature + salinity; one 20—30°C and one 30—35°C, and predictions were made for effective quantum yield = 0 (Tables 6–9). This may be less useful since only one of the predictions from this analysis was from within the range of experimental variables.

The reduced effective quantum yield was observed across the experimental period at the highest salinities (e.g. at 20°C, Figure 8a) but not at lower salinities (Figure 8a). A negative response to salinity was most obvious in the 140 ppt (i.e. highest) treatment where reduced plant photosynthesis measured as effective quantum yield approached zero. The overall observed change to net weight change (Figure 9) was principally derived from the filamentous algal response to salinity with temperature serving to modify rates of change following the models already described.

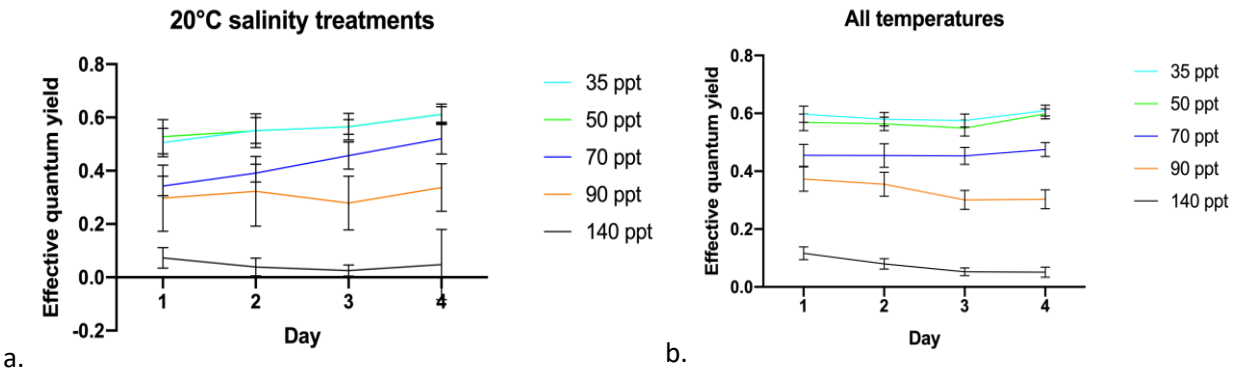

Figure 8. Daily measurements of the effective quantum yield ($ø_{PSII}$) of filamentous algae. a) 20°C temperature treatment grown under varying salinities ± 95% CI. b) average across all temperature treatments ± 95% CI.

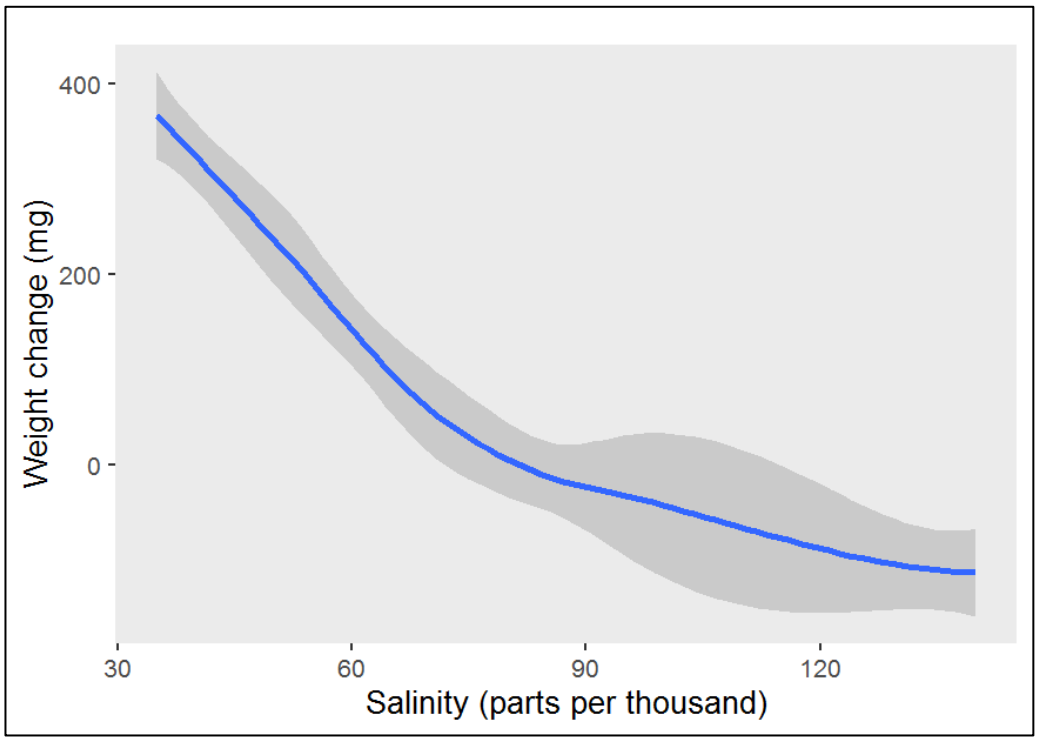

Figure 9. Smoothed trend line of the weight change associated with salinity at all temperatures. The grey bands represent the 95% confidence interval of the mean which is represented by the blue line.

3.2 Predictions for thresholds of change

Filamentous algae exhibited zero net weight gain and zero net Quantum yield based on varying experimental conditions of temperature and salinity models. These results were used to develop, based on models described above and the experimental data, estimates of the parameters which will lead to algal growth reaching zero or negative growth. As stated, these values should be considered to have greater statistical support when within the range of observations. Notably, at lower temperatures, algal growth does not reach a predicted zero or negative growth until over 85 ppt salinity (i.e. 20-25°C), and over 110 ppt at 30°C.

Table 2. Levels of salinity predicted to cause net weight change to be zero up to temperatures of 30°C.

Temperature (°C)	Salinity at which weight change = 0 (ppt)
20	86.039 (within range of observations)
25	99.672 (within range of observations)
30	113.304 (within range of observations)

Table 3. Temperatures predicted to cause net weight change to be zero up to temperatures of 30°C.

Salinity (ppt)	Temperature (°C)
50	6.782 (outside range of observations)
70	-14.117 (outside range of observations)
90	-21.45 (outside range of observations)
140	-39.79 (outside range of observations)

Table 4. Levels of salinity predicted to cause net weight change to be zero up to temperatures of 30°C.

Temperature (°C)	Salinity at which weight change = 0 (ppt)
30	107.817 (within range of observations)
35	99.318 (within range of observations)

Table 5. Temperatures predicted to cause net weight change to be zero up to temperatures of 30°C.

Salinity (ppt)	Temperature (°C)
50	62.46 (outside range of observations)
70	52.25 (outside range of observations)
90	40.48 (outside range of observations)
140	11.07 (outside range of observations)

Table 6. Levels of salinity predicted to cause effective quantum yield, to be zero up to temperatures of 30°C.

Temperature (°C)	Salinity at which effective quantum yield = 0 (ppt)
20	154.4 (outside range of observations)
25	164.4 (outside range of observations)
30	174.4 (outside range of observations)

Table 7. Temperatures predicted to cause effective quantum yield, zero up to temperatures of 30°C.

Salinity (ppt)	Temperature (°C)
50	32.2 (outside range of observations)
70	22.2 (within range of observations)
90	12.2 (outside range of observations)
140	-12.8 (outside range of observations)

Table 8. Levels of salinity predicted to cause effective quantum yield, zero up to temperatures above 30°C.

Temperature (°C)	Salinity at which yield = 0 (ppt)
30	181.6 (outside range of observations)
35	168.6 (outside range of observations)

Table 9. Temperatures predicted to cause effective quantum yield, to be = 0, above 30°C.

Salinity (ppt)	Temperature (°C)
50	80.62 (outside range of observations)
70	72.92 (outside range of observations)
90	65.23 (outside range of observations)
140	46.0 (outside range of observations)

3.3 Field measurements of temperature

Variation in temperature over diurnal cycles and within season for the October-December period are summarised in Figure 10 and Table 10. The range of temperatures across all sites are within the experimental treatments applied in these experiments.

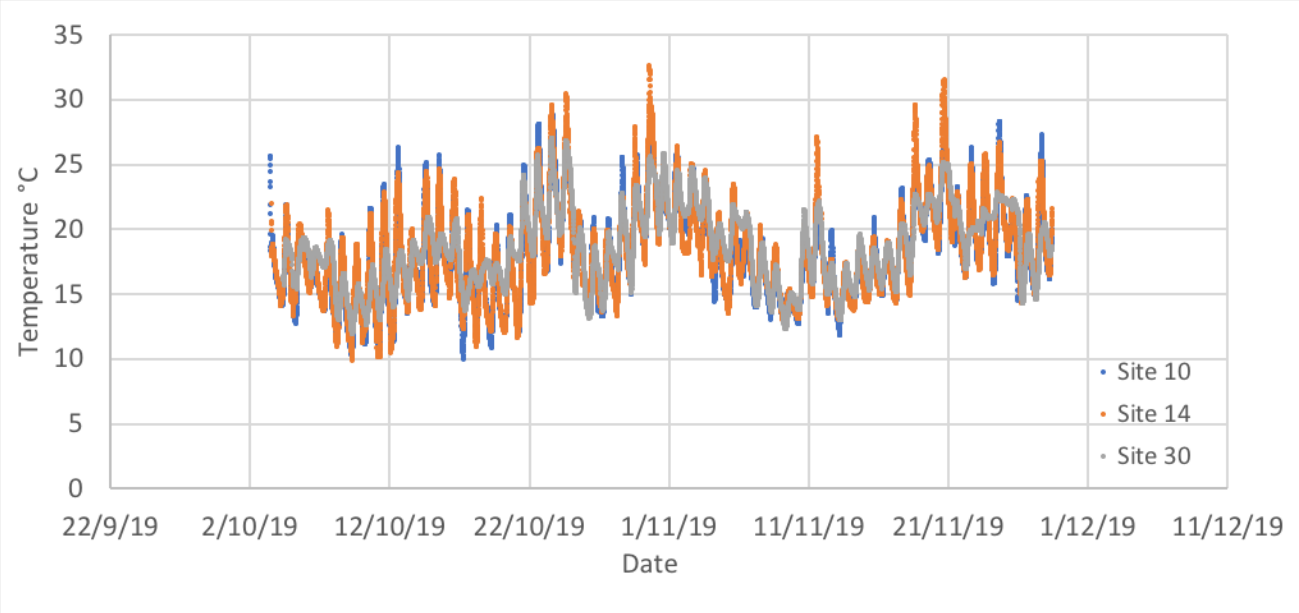

Figure 10. Temperature logger data from field deployed HOBO Pendant MX Water Temperature Loggers (HOBO MX2201) at three field sites in southern Coorong (refer to Figure 1 for locations).

Table 10. Summary of temperature logger data characteristics from three field sites in the central and southern Coorong (refer to Figure 1 for locations).

	Unit	Site 10	Site 14	Site 30
N		16118	16115	15893
Mean	Temperature (°C)	17.99	18.20	18.58
Std. Error of Mean	Temperature (°C)	0.029	0.030	0.024
Range	Temperature (°C)	18.79	22.70	15.14
Minimum	Temperature (°C)	9.95	9.86	11.88
Maximum	Temperature (°C)	28.74	32.56	27.02
Percentiles	25^{th}	15.18	15.31	16.34
	50^{th}	17.67	17.76	18.40
	75^{th}	20.29	20.55	20.80

4 Discussion

These experimental results extend our understanding of the growth responses and thresholds of change for filamentous green algae that form blooms in the southern Coorong, specifically the interaction between algal growth, temperature and salinity. From previous data sets, water temperature was known to affect algal growth rates. The optimum temperature for the *Ulva paradoxa* filamentous green algal community utilised in these experiments appears to be 30°C, that is the temperature where the relationship between net weight gain is the most positive up to 90 ppt salinity. At a salinity of 140 ppt the growth of algae is inhibited at all temperatures. Compared to the majority of studies published on other *Ulva* species, the optimum growth temperatures occur in the range of 10 – 20°C (summarised in Table 8, Collier et al. 2017). However, *U. linza*, which has been seen to form the green tide blooms in the Yellow Sea, was determined to have had an optimum growth temperature at 20 – 30°C (Kim et al. 2011).

Limitations on interpreting the effect of these results relate to the potential influence of lower nutrients on filamentous green algal growth. These experiments were conducted at relatively high levels of nitrogen availability, determined previously to be enabling of algal growth at different salinities (Collier et al. 2017). For this reason, the experimental results generated should be considered in conjunction with the result from previous experiments where the relationship between algal growth and salinity were assessed under different nutrient regimes; in particular, experimental results testing thresholds of algal growth under differing salinities, as described in Collier et al. (2017).

Modelling of statistical outcomes lead to the following conclusions:

- Growth rates peak at 30°C and salinity of 90 ppt.
- At salinities less than 90ppt, algae gowth rates increase positively in response to temperature up to 30°C.

During the two months of field deployment of *in situ* loggers, shallow water temperatures did not exceed the range tested experimentally here. For the three locations across the central and southern Coorong that loggers were deployed, surface forming filamentous algal blooms were seen forming in the system during October – December 2019, across the range of temperatures that were logged.

It is clear that local salinity in places where the algae are growing has a strong effect on filamentous algal bloom formations to the scale seen in the southern Coorong.

The new information on the interactive effects of temperature and salinity on algal growth, in conjunction with previous data showing the impact of nutrients on algal growth in Collier et al. (2017) will enable updated models to be implemented for ongoing research and decision making in the Coorong (Table 11).

Table 11. Outcomes from the data presented in this study and the potential to provide updates to the hydrodynamic biogeochemical model and its configuration as presented in Collier et al. (2017).

Filamentous Algae parameterisation (NA = not applicable to available data sets)				
Model parameter (and notation)	Description of model parameter	Unit	Current model	Potential update applicable
$RgrowtFA_h$	Maximum FA growth rate at 20□C	d-1	0.33	Value can now be updated for a wider range of temperatures and an independent test of growth rate can be achieved from the data collected
I_K	Light intensity for maximum production (before photo-inhibition effects)	µE m-2 s-1	300	NA

$KeFA$	Light attenuation over the depth of the plant (within the canopy)	(m-1) (g m-2)-1		Experimental data from shading experiments can be applied. Field data still needs collecting.
$\vartheta growtFA h$	Arrhenius temperature scaling for growth	-	1.08	Can be updated with experimental data relationships from this study.
T_{std}	Standard temperature	Temperature (°C)	20	As above
$Topt$	Optimum temperature	Temperature (°C)	27	As above
$Tmax$	Maximum temperature	Temperature (°C)	37	As above
$SmaxFA$	Upper salinity limit before increased mortality	g L^{-1}	50	As above
$S_{min}FA$	Lower salinity limit before increased mortality	g L^{-1}	20	As above
min_S	Minimum salinity tolerance	g L^{-1}	5	As above
max_S	Maximum salinity tolerance	g L^{-1}	80	As above
$RrespFA$	Filamentous algae respiration rate at 20□C	d^{-1}	0.020	As above
τ_c	Critical shear stress for sloughing / detachment	N m^{-2}	0.05	Preliminary field observations can be applied

Finally, testing of growth parameters coupled with field observations on this algal community remains an important component of understanding the dynamics of the Coorong ecosystem. This is principally because the extrapolation of data from studies elsewhere is problematic due to the hypersaline conditions and the clear adaptation of the plants to the extreme conditions they occupy. As models require thresholds to be determined ongoing testing of filamentous algal thresholds for growth rates, the impact of algal shading on *Ruppia* growth and turnover of total filamentous algal biomass may need to be parameterised.

References

Coffaro, G, and Sfriso, A (1997) Simulation model of *Ulva rigida* growth in shallow water of the Lagoon of Venice. Ecological Modelling 102: 55-66.

Collier, C., van Dijk, K.-J., Erftemeijer, P., Foster, N., Hipsey, M., O'Loughlin, E., Ticli, K. and Waycott, M. (2017) Optimising Coorong Ruppia habitat: Strategies to improve habitat conditions for *Ruppia tuberosa* in the Coorong (South Australia) based on literature review, manipulative experiments and predictive modelling. M. Waycott, Ed. Report to Department of Environment and Natural Resources (DEWNR). Adelaide, South Australia, University of Adelaide, School of Biological Sciences. A University of Adelaide and State Herbarium of South Australia, South Australia, 169 pp.

Cummins, S P, Roberts, D E and Zimmerman, K D (2004) Effects of the green macroalga *Enteromorpha intestinalis* on macrobenthic and seagrass assemblages in a shallow coastal estuary. Marine Ecology Progress Series 266: 77-87.

Frahn, K, and Gehrig, S L (2015) Distribution and abundance of *Ruppia tuberosa* in the Coorong, December 2014. South Australian Research and Development Institute (Aquatic Sciences), Adelaide.

Frahn, K, Nicol, J and Strawbridge, A (2012) Current distribution and abundance of *Ruppia tuberosa* in the Coorong. South Australian Research and Development Institute (Aquatic Sciences), Adelaide. SARDI Publication No. F2012/000074-1. SARDI Research Report Series No. 615. 22 pp.

Han, Q, and Liu, D (2014) Macroalgae blooms and their effects on seagrass ecosystems. Journal of Ocean University of China 13: 791-798.

Han, Q, Soissons, L M, Bouma, T J, van Katwijk, M M and Liu, D (2016) Combined nutrient and macroalgae loads lead to response in seagrass indicator properties. Marine Pollution Bulletin 106:174-182.

Hipsey, M R, Busch, B D and Katumba, G (2016) CLLMM Water Quality Response Model v1: Model overview and parameterisation approach. AED Report #R31, The University of Western Australia, Perth, Australia. 58 pp.

Holmer, M, and Nielsen, R M (2007) Effects of filamentous algal mats on sulfide invasion in eelgrass (*Zostera marina*). Journal of Experimental Marine Biology and Ecology **353**: 245-252.

Kim, D, Aldridge, K T, Ganf, G G and Brookes, J D (2015) Physicochemical influences on *Ruppia tuberosa* abundance and distribution mediated through life cycle stages. Inland Waters **5**: 451-460.

Lavery, P S and McComb, A J (1991) The nutritional eco-physiology of *Chaetomorpha linum* and *Ulva rigida* in Peel Inlet, Western Australia. Botanica Marina, 34: 251-260.

McGlathery, K J, Sundbäck, K and Anderson, I C (2007). Eutrophication in shallow coastal bays and lagoons: the role of plants in the coastal filter. Marine Ecology Progress Series **348**:1-18.

Muggeo, V M R (2008) Segmented: an R Package to Fit Regression Models with Broken-Line Relationships. R News, 8/1, 20-25. URL https://cran.r-project.org/doc/Rnews/.

Nelson, W A, Neill, K F, D'Archino R (2015) When seaweeds go bad: an overview of outbreaks of nuisance quantities of marine macroalgae in New Zealand, New Zealand Journal of Marine and Freshwater Research, 49: 472-491

Osterling, M, and Pihl, L (2001) Effects of filamentous green algal mats on benthic macrofaunal functional feeding groups. Journal of Experimental Marine Biology and Ecology 262: 159 - 183.

Paton, D C (2010) At the end of the river: the Coorong and Lower Lakes. by ATF Press.

Paton, D C, McKillop, T and Bailey, C P (2011) Developing ecological knowledge to inform the reestablishment of *Ruppia tuberosa* in the southern Coorong. University of Adelaide, Adelaide.

Paton, D C, Paton, F L and Bailey, C P (2017) Monitoring of *Ruppia tuberosa* in the southern Coorong, summer 2016-17. University of Adelaide, Adelaide.

Paton, D C, Rogers, D J, Aldridge, K, Deegan, B and Brookes, J (2009) A future for the Coorong and Lower Lakes. Pacific Conservation Biology 15: 7-10.

Pedersen, M F, and Borum, J (1996) Nutrient control of algal growth in estuarine waters. Nutrient limitation and the importance of nitrogen requirements and nitrogen storage among phytoplankton and species of macroalgae. Marine Ecology Progress Series 142: 261-272.

Tweedley, J R M, Jackson, E L, and Attrill M J (2008) *Zostera marina* seagrass beds enhance the attachment of the invasive alga Sargassum *muticum* in soft sediment. Marine Ecology Progress Series 354: 305309.

Wickham H, Miller E (2019) Haven: Import and Export 'SPSS', 'Stata' and 'SAS' Files. R package version 2.2.0. https://CRAN.R-project.org/package=haven

Womersley, H B S (1975) Plant life of the Coorong Lagoons. In: Noye, J (Ed), The Coorong. The University of Adelaide, Adelaide.

Appendix A – Statistical outputs

Statistical analysis outcomes of filamentous algal growth under varying salinity and temperature

Two linear predictive models for weight change were resolved, one for data up to and including 30°C and another for data 30°C and up. The negative impact of treatment on filamentous algae were taken to be where the *net weight change* is equal to zero or negative and *effective quantum yield* is equal to zero or negative, is predicted for every possible scenario in these data (Tables A1—A4; A5—A9). This was done because there were significant interactions between the temperatures at which the observations were made and salinity (Table A12), and there was a non-linear effect in the data, but either side of the turning point, there are strong linear relationships. Also, fitting a generalised additive model is not possible. A term (temperature) has fewer unique covariate combinations than specified maximum degrees of freedom, since temperature readings were made at 20, 25, 30, and 35°C only. In addition, two linear models and a set of tables of predictions have been made for the modelled mean yield ~ temperature + salinity, and these follow the method for the weight change models.

The model outcomes were derived as formulas:

For temperatures 20—30°C:

The weight change = 139.671 – 4.433(salinity) + 12.087(temperature) For

temperatures 30—35°C:

The weight change = 838.999 – 5.283(salinity) – 8.98(temperature)

These formulas were then used to determine the different predicted scenarios which result in weight change = 0, and the results given in Tables 1—4, but it must be noted that only predictions made from within the range of experimental variables can be considered.

In addition, two linear models were developed for Quantum yield x temperature + salinity, one 20—30°C and one 30—35°C, and predictions made for Quantum yield = 0 (Tables 5—8). This may be less useful since only one of the predictions from this analysis was from within the range of experimental variables.

Table A0. The break point modelling in the segmented package, determined to be 29.427°C.

```
      ***Regression Model with Segmented Relationship(s)***
Call:
segmented.lm(obj = lin.mod, seg.Z = ~temperature, npsi = 1)
Estimated       Break-Point(s):
Est.   St.Err   psi1.temperature
29.427  1.253

Meaningful coefficients of the linear terms:
               Estimate Std. Error t value Pr(>|t|)
(Intercept)      4.4364   161.0874   0.028 0.978159
temperature     26.3469     6.9628   3.784 0.000483 ***
salinity        -8.4906     0.7454 -11.391    2e-14 ***
U1.temperature -44.8594     9.3530  -4.796       NA
---
Signif. codes:  0 ‘***’ 0.001 ‘**’ 0.01 ‘*’ 0.05 ‘.’ 0.1 ‘ ’ 1
Residual standard error: 79.61 on 42 degrees of freedom
Multiple R-Squared: 0.7919,  Adjusted R-squared: 0.7721
Convergence attained in 2 iter. (rel. change 0)
```

Predictions from the two weight change models

Table A1. Levels of salinity predicted to cause weight change to be = 0 up to 30°C

Temperature (°C)	Salinity at which weight change = 0 (ppt)
20	86.039 (within range of observations)
25	99.672 (within range of observations)
30	113.304 (within range of observations)

Table A2. Temperatures predicted to cause weight change to be = 0, up to 30°C

Salinity (ppt)	Temperature (°C)
50	6.782 (outside range of observations)
70	-14.117 (outside range of observations)
90	-21.45 (outside range of observations)
140	-39.79 (outside range of observations)

Table A3. Levels of salinity predicted to cause weight change to be = 0 above 30°C

Temperature (°C)	Salinity at which weight change = 0 (ppt)
30	107.817 (within range of observations)
35	99.318 (within range of observations)

Table A4. Temperatures predicted to cause weight change to be = 0, above 30°C

Salinity (ppt)	Temperature (°C)
50	62.46 (outside range of observations)
70	52.25 (outside range of observations)
90	40.48 (outside range of observations)
140	11.07 (outside range of observations)

Summary of the two models

Model and predictions for yield ~ salinity + temperatures

Predictions from the two models

Table A5. Levels of salinity predicted to cause yield to be = 0 up to 30°C.

Temperature (°C)	Salinity at which yield = 0 (ppt)
20	154.4 (outside range of observations)
25	164.4 (outside range of observations)
30	174.4 (outside range of observations)

Table A6. Temperatures predicted to cause yield to be = 0, up to 30°C.

Salinity (ppt)	Temperature (°C)
50	32.2 (outside range of observations)
70	22.2 (within range of observations)

90	12.2 (outside range of observations)
140	-12.8 (outside range of observations)

Table A7. Levels of salinity predicted to cause yield to be = 0 above 30°C.

Temperature (°C)	Salinity at which yield = 0 (ppt)
30	181.6 (outside range of observations)
35	168.6 (outside range of observations)

Table A8. Temperatures predicted to cause yield to be = 0, above 30°C.

Salinity (ppt)	Temperature (°C)
50	80.62 (outside range of observations)
70	72.92 (outside range of observations)
90	65.23 (outside range of observations)
140	46.0 (outside range of observations)

Table A9. Model for mean yield ~ salinity + temperature for temperatures up to 30°C.

```
> summary(model1)

Call:
lm(formula = meanY ~ salinity + temperature, data = b)
Residuals:
     Min       1Q   Median       3Q      Max
-0.14490 -0.04358 -0.00982  0.03600  0.18085

Coefficients:
             Estimate  Std.  Error  t  value  Pr(>|t|)
(Intercept)  0.5721136  0.0354052  16.159  < 2e-16 ***
salinity    -0.0053394  0.0001478 -36.120  < 2e-16 ***
temperature  0.0102419  0.0013235   7.738 3.93e-12 ***
---
Signif. codes:  0 ‘***’ 0.001 ‘**’ 0.01 ‘*’ 0.05 ‘.’ 0.1 ‘ ’ 1
Residual standard error: 0.05919 on 117 degrees of freedom
Multiple R-squared:  0.921, Adjusted R-squared:  0.9197
F-statistic: 682.3 on 2 and 117 DF,  p-value: < 2.2e-16
```

Table A10. Formula for yield ~ salinity + temperature for temperatures up to 30°C.

```
"y = 0.572 - 0.005 * salinity + 0.01 * temperature"
```

Table A11. Model for mean yield ~ salinity + temperature for temperatures from 30°C upwards.

```
> summary(model1)

Call:
lm(formula = meanY ~ salinity + temperature, data = b)
Residuals:
      Min        1Q    Median        3Q       Max  -
0.139374 -0.038678  0.000158  0.036011  0.104464

Coefficients:
             Estimate  Std.  Error  t  value  Pr(>|t|)
(Intercept)  1.297914   0.072392  17.929  < 2e-16 ***
salinity    -0.005327   0.000150 -35.521  < 2e-16 ***
temperature -0.013475   0.002192  -6.146 3.27e-08 ***
---
Signif. codes:  0 ‘***’ 0.001 ‘**’ 0.01 ‘*’ 0.05 ‘.’ 0.1 ‘ ’ 1
Residual standard error: 0.04902 on 77 degrees of freedom
Multiple R-squared:  0.9441, Adjusted R-squared:  0.9426
F-statistic: 649.7 on 2 and 77 DF,  p-value: < 2.2e-16
```

Table A12. Formula for yield ~ salinity + temperature for temperatures from 30°C upwards.

```
"y = 1.298 - 0.005 * salinity - 0.013 * temperature"
```

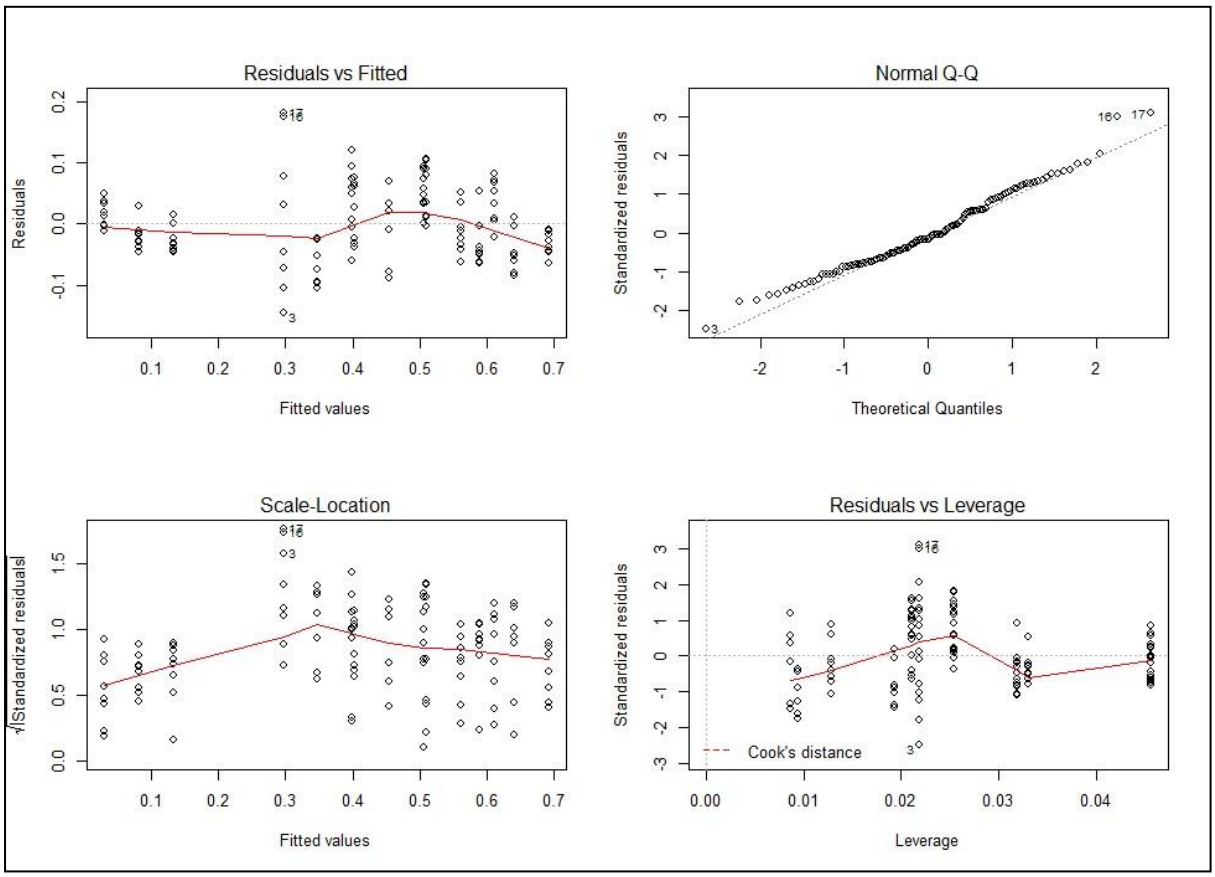

Figure A1. Diagnostic plots for model for mean yield ~ salinity + temperature for temperatures up to 30°C.

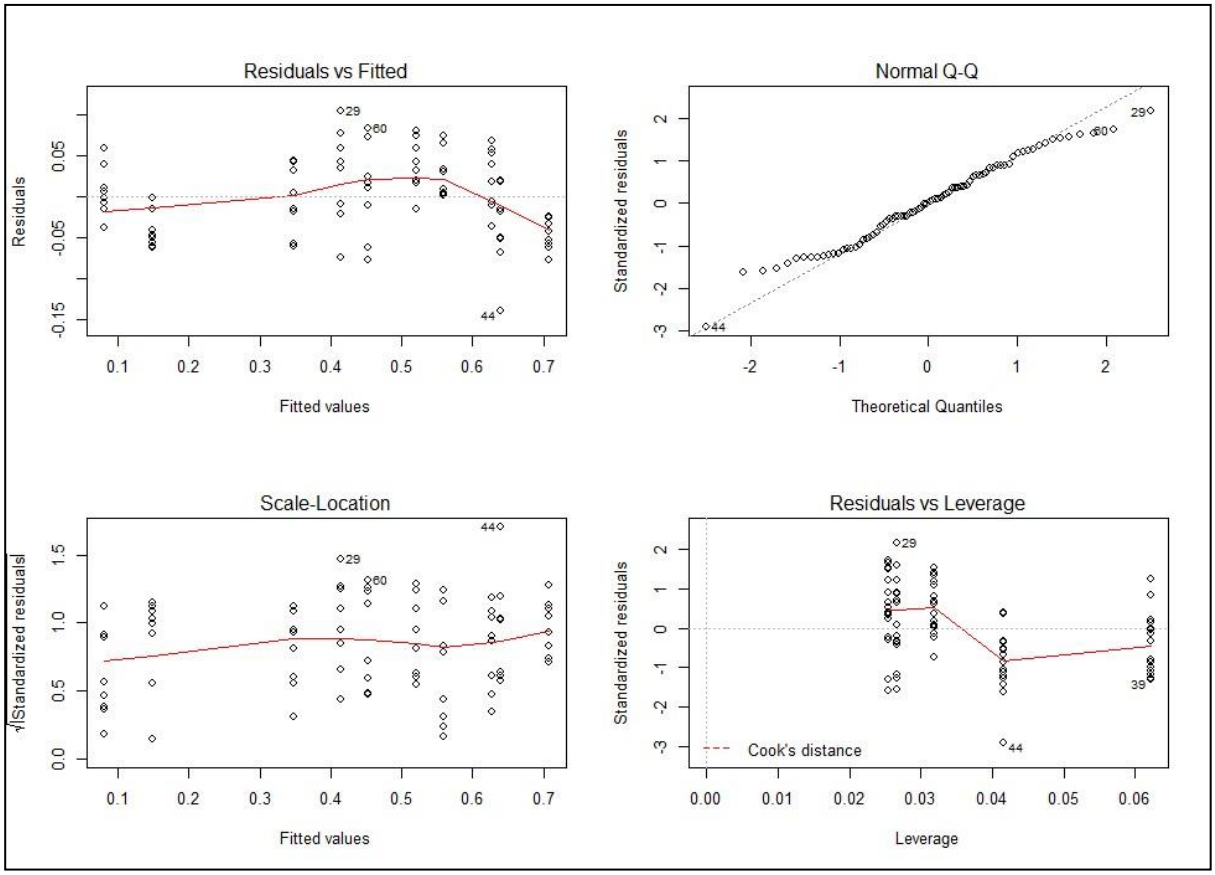

Figure A2. Diagnostic plots for model for mean yield ~ salinity + temperature for temperatures from 30°C upwards.

Interaction between temperature and salinity

Plots of weight change ~ salinity + temperature (Figure 3A and 4A) suggest that there is some interaction between temperature and salinity, and this interactions was modelled (Table 13). All interactions are significant, and this means that as salinity changes, there is a changing reaction to temperature.

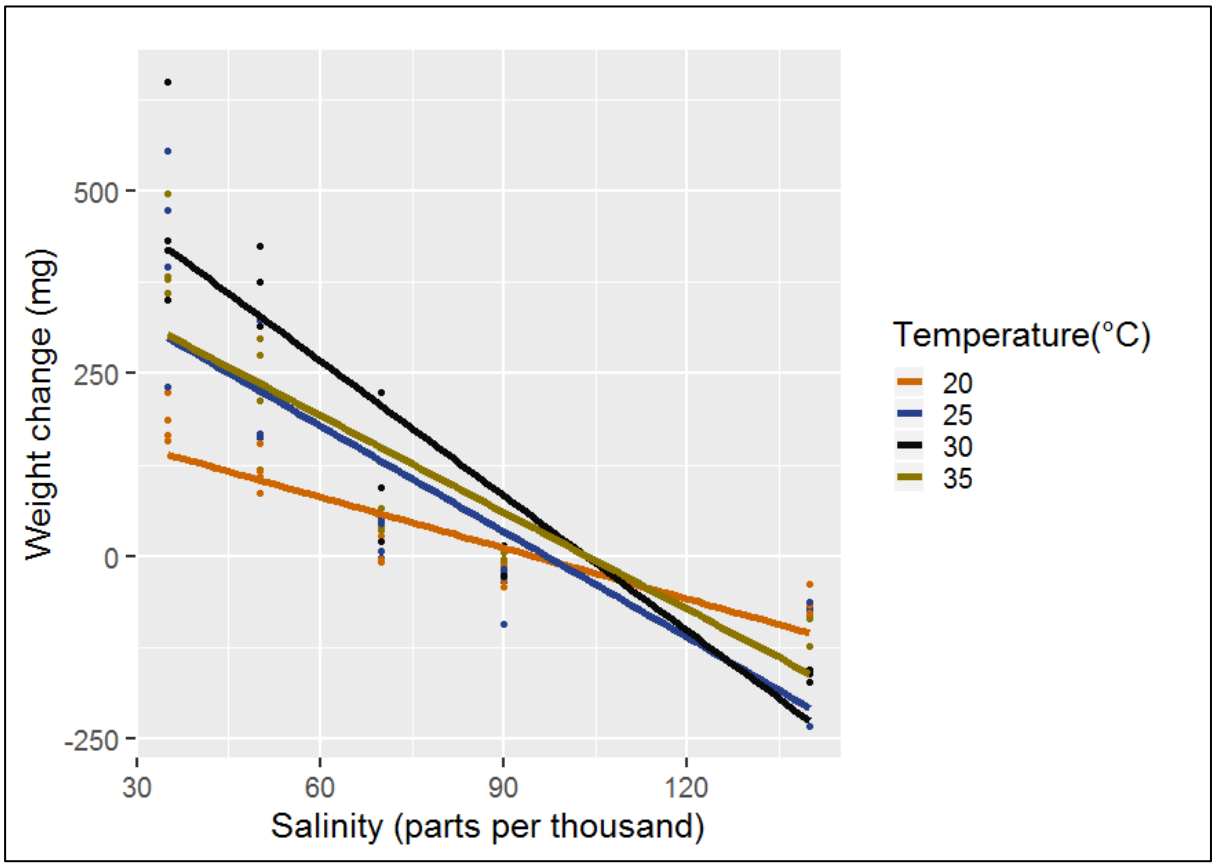

Figure A3. Plot of the weight change associated with salinity at specific temperatures shows potential interaction in this figure. This interaction was modelled and is significant.

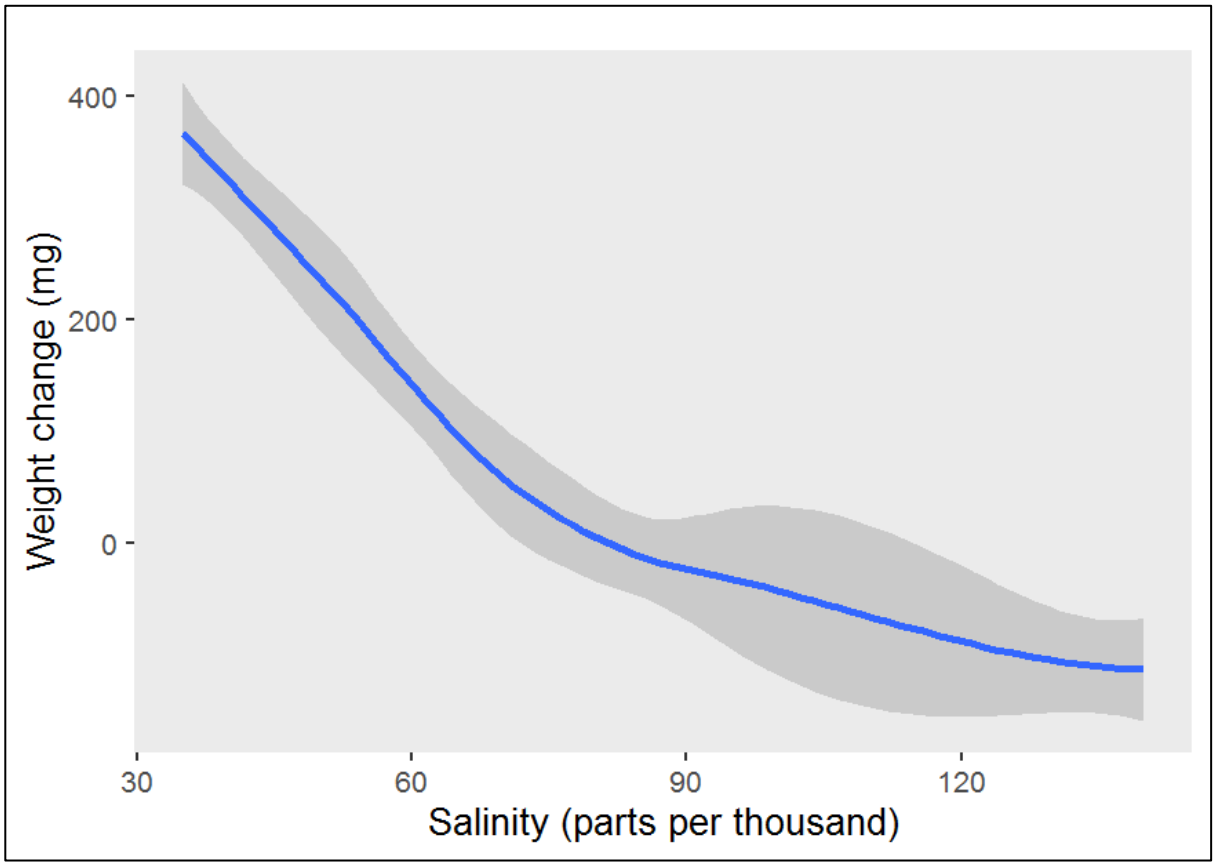

Figure A4. A plot featuring loess smoothed trend line of the weight change associated with salinity at all temperatures shows that increasing salinity is correlated with reduction in weight. The grey bands represent the 95% confidence interval of the mean which is represented by the blue line.

Table A13. Interaction of salinity and temperature in the weight change ~salinity + temperature model. All interactions are significant.

```
> summary(model3)
 Call: lm(formula = weight_change ~ salinity + temperature +
salinity *      temperature, data = W)

Residuals:
     Min       1Q   Median       3Q      Max
-185.373  -65.244   -7.591   62.295  254.668

Coefficients:
                        Estimate  Std.  Error  t  value  Pr(>|t|)
(Intercept)              220.8859    47.7878    4.622 1.63e-05 ***
salinity                  -2.3238     0.5607  -4.145 9.16e-05 ***
temperature25            247.0702    67.5822    3.656 0.000484 ***
temperature30            415.8483    67.5822    6.153 3.85e-08 ***
temperature35            236.6842    67.5822    3.502 0.000797 ***
salinity:temperature25   -2.4958     0.7929   -3.148 0.002395 **
salinity:temperature30   -3.8308     0.7929   -4.831 7.42e-06 ***
salinity:temperature35   -2.0871     0.7929  -2.632 0.010371 *
---
```

```
Signif. codes:  0 ‘***’ 0.001 ‘**’ 0.01 ‘*’ 0.05 ‘.’ 0.1 ‘ ’ 1

Residual standard error: 91.65 on 72 degrees of freedom
Multiple R-squared:  0.8019,      Adjusted R-squared:  0.7826
F-statistic: 41.64 on 7 and 72 DF,  p-value: < 2.2e-16
```

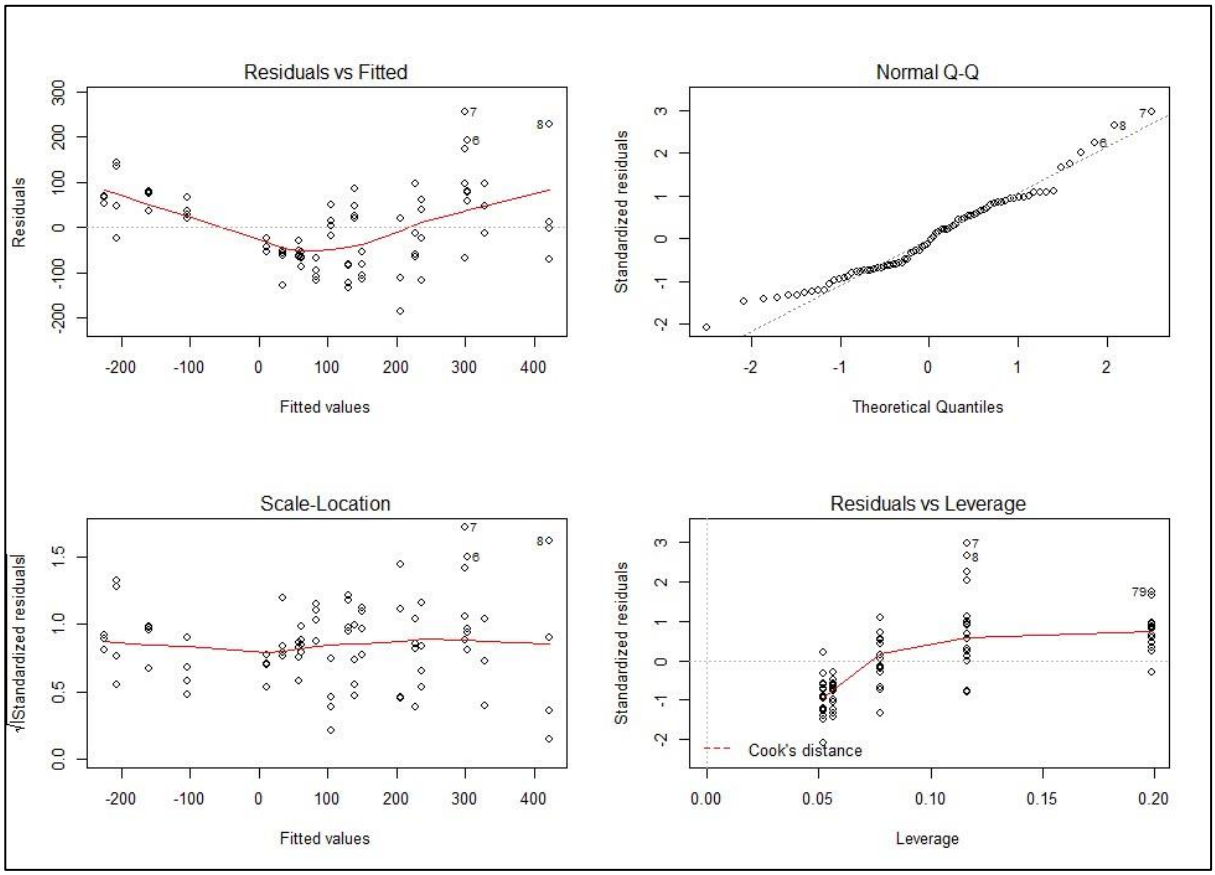

Figure A5. Diagnostic plots for model for weight change ~ salinity + temperature + salinity*temperature.

Additional plots

The additional plots show reaction of weight change at a fixed temperature to varying salinity, and reactions of weight change at a fixed salinity to varying temperature.

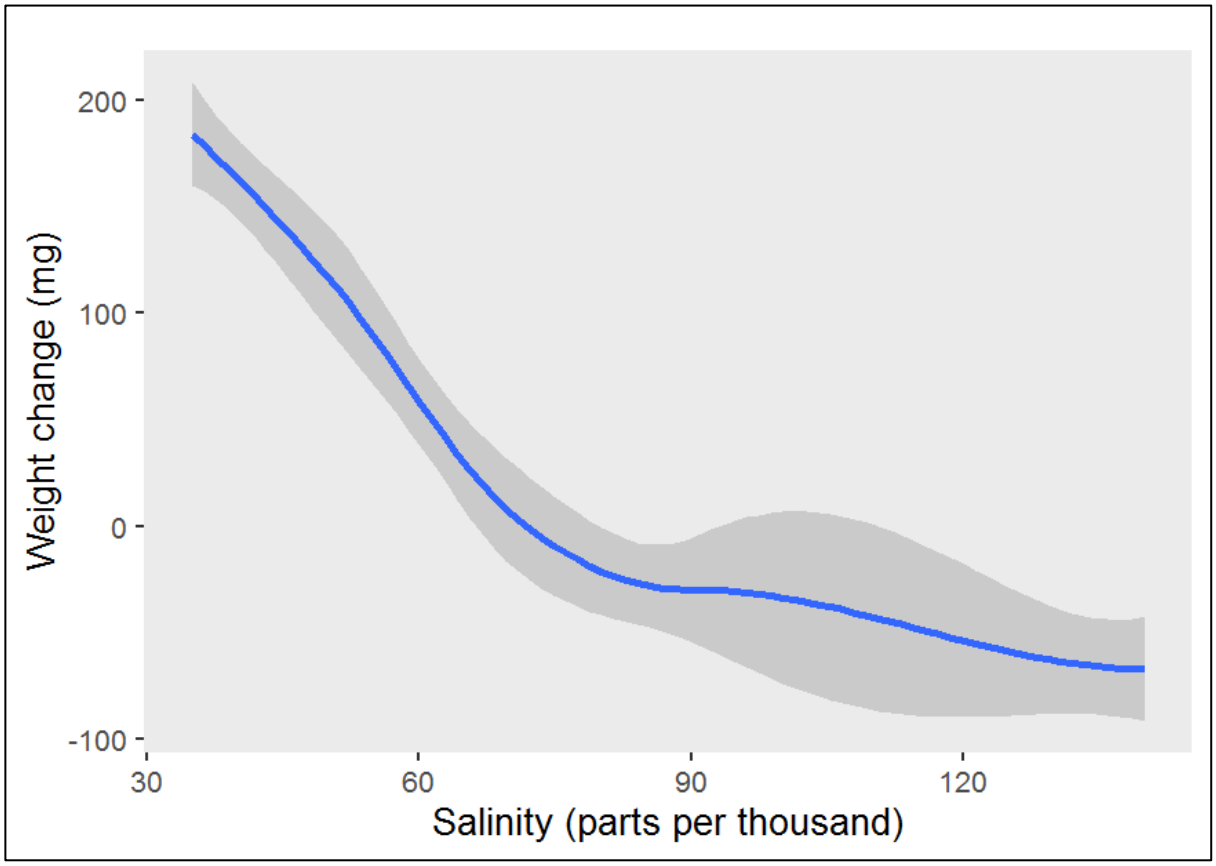

Figure A6. Weight change response associated with changing salinity at 20°C. The blue line represents the loess smoothed mean estimate and the grey band represents the 95% confidence interval of this estimate.

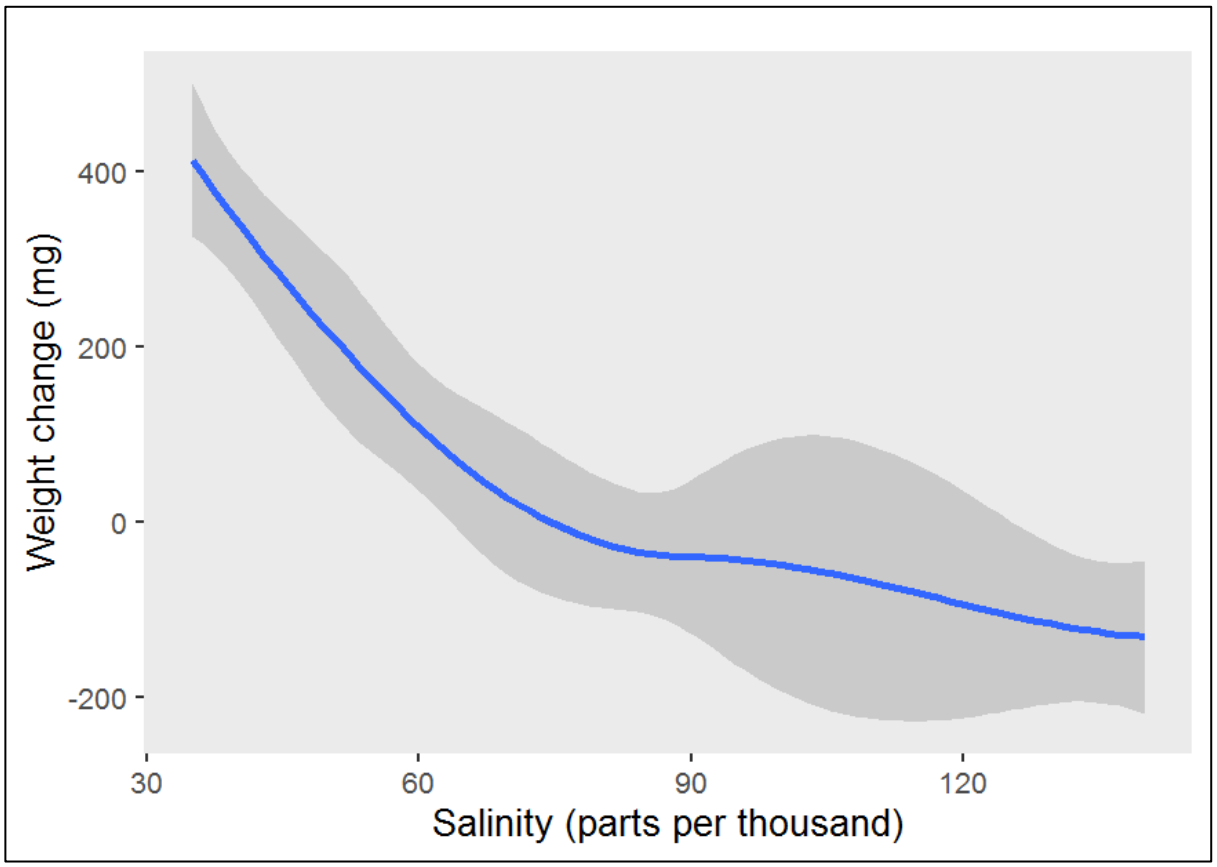

Figure A7. Weight change response associated with changing salinity at 25°C. The blue line represents the loess smoothed mean estimate and the grey band represents the 95% confidence interval of this estimate.

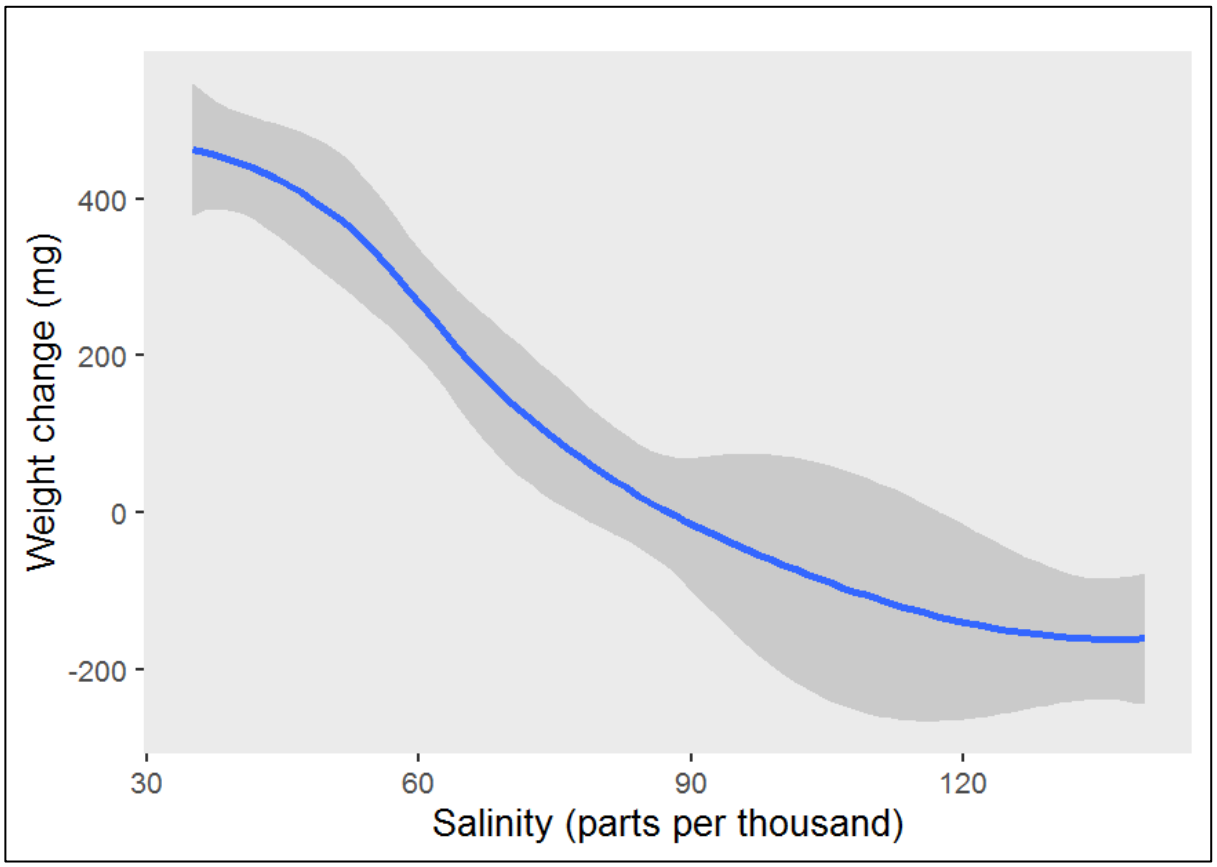

Figure A8. Weight change response associated with changing salinity at 30°C. The blue line represents the loess smoothed mean estimate and the grey band represents the 95% confidence interval of this estimate.

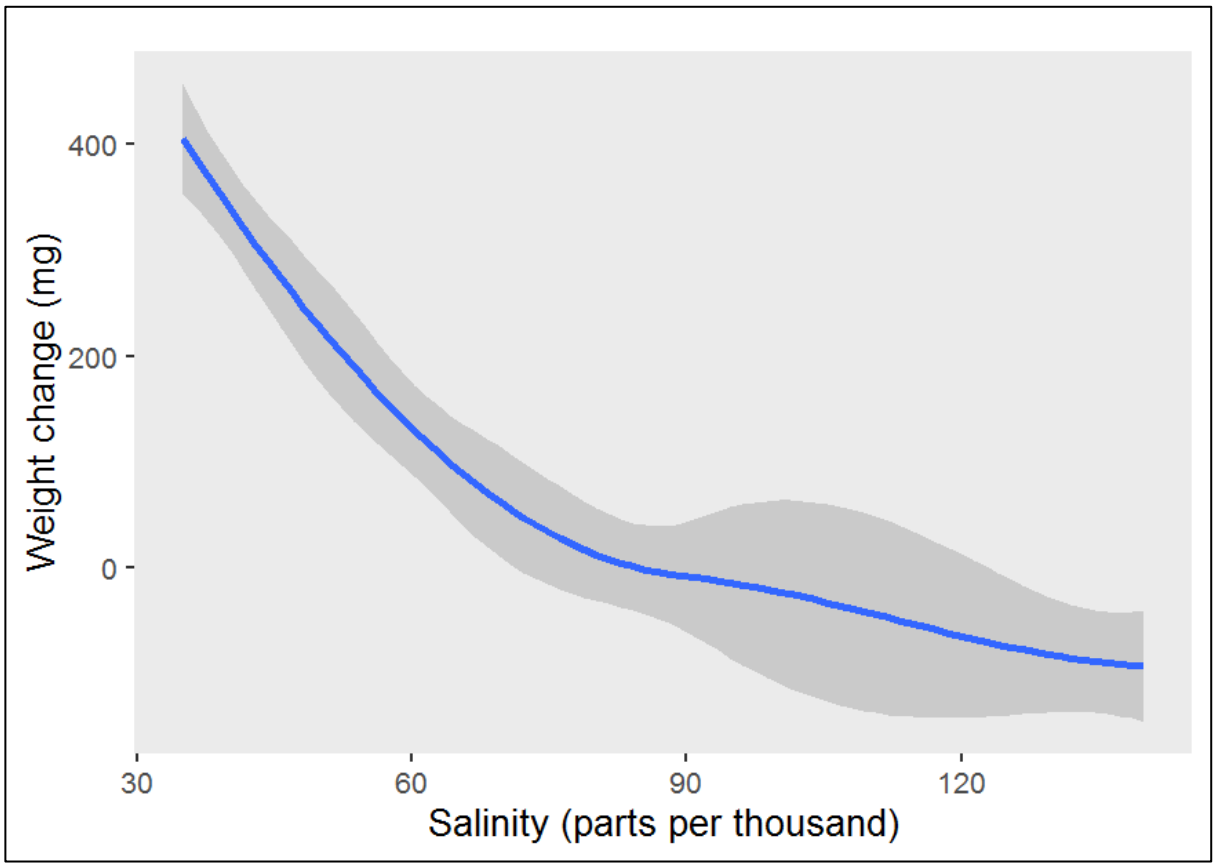

Figure A9. Weight change response associated with changing salinity at 35°C. The blue line represents the loess smoothed mean estimate and the grey band represents the 95% confidence interval of this estimate.

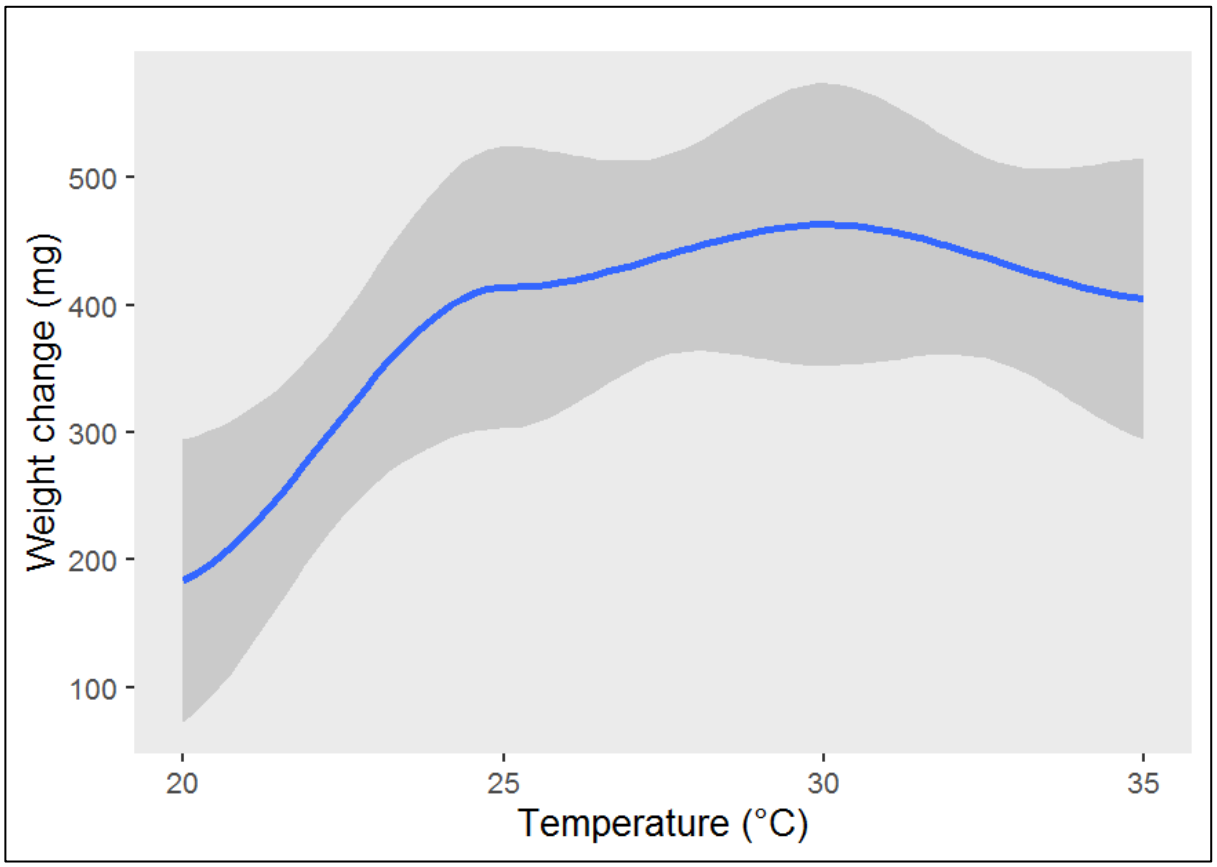

Figure A10. Weight change response associated with changing temperature at 35 parts per-thousand salinity. The blue line represents the loess smoothed mean estimate and the grey band represents the 95% confidence interval of this estimate.

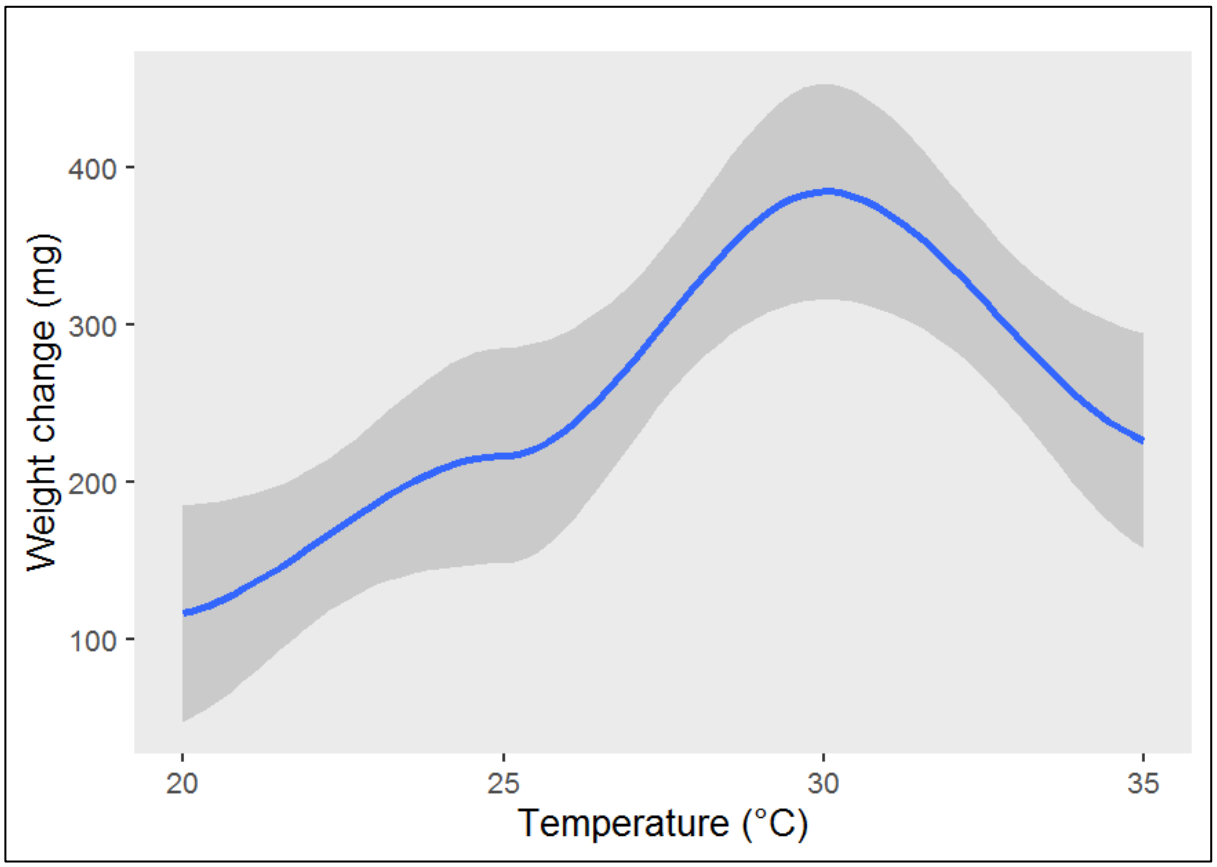

Figure A11. Weight change response associated with changing temperature at 50 parts per-thousand salinity. The blue line represents the loess smoothed mean estimate and the grey band represents the 95% confidence interval of this estimate.

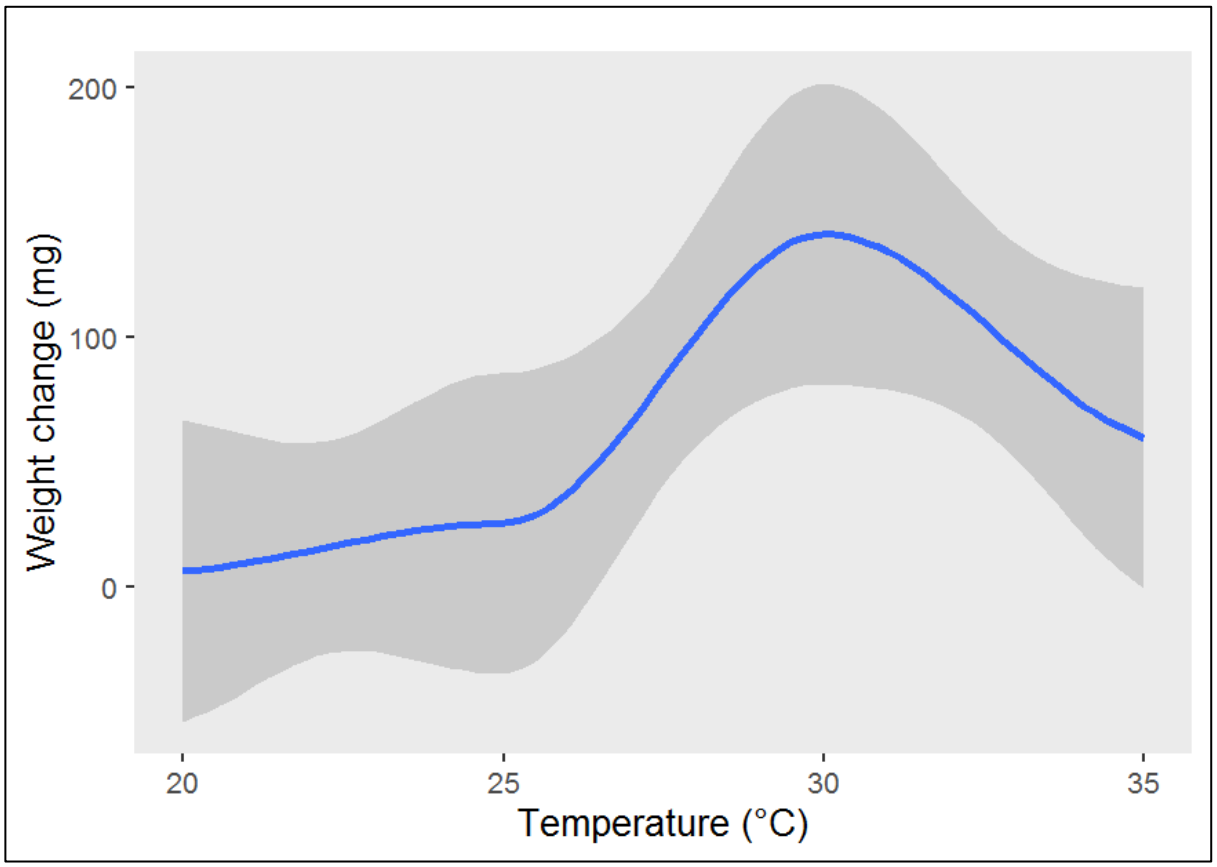

Figure A12. Weight change response associated with changing temperature at 70 parts per-thousand salinity. The blue line represents the loess smoothed mean estimate and the grey band represents the 95% confidence interval of this estimate.

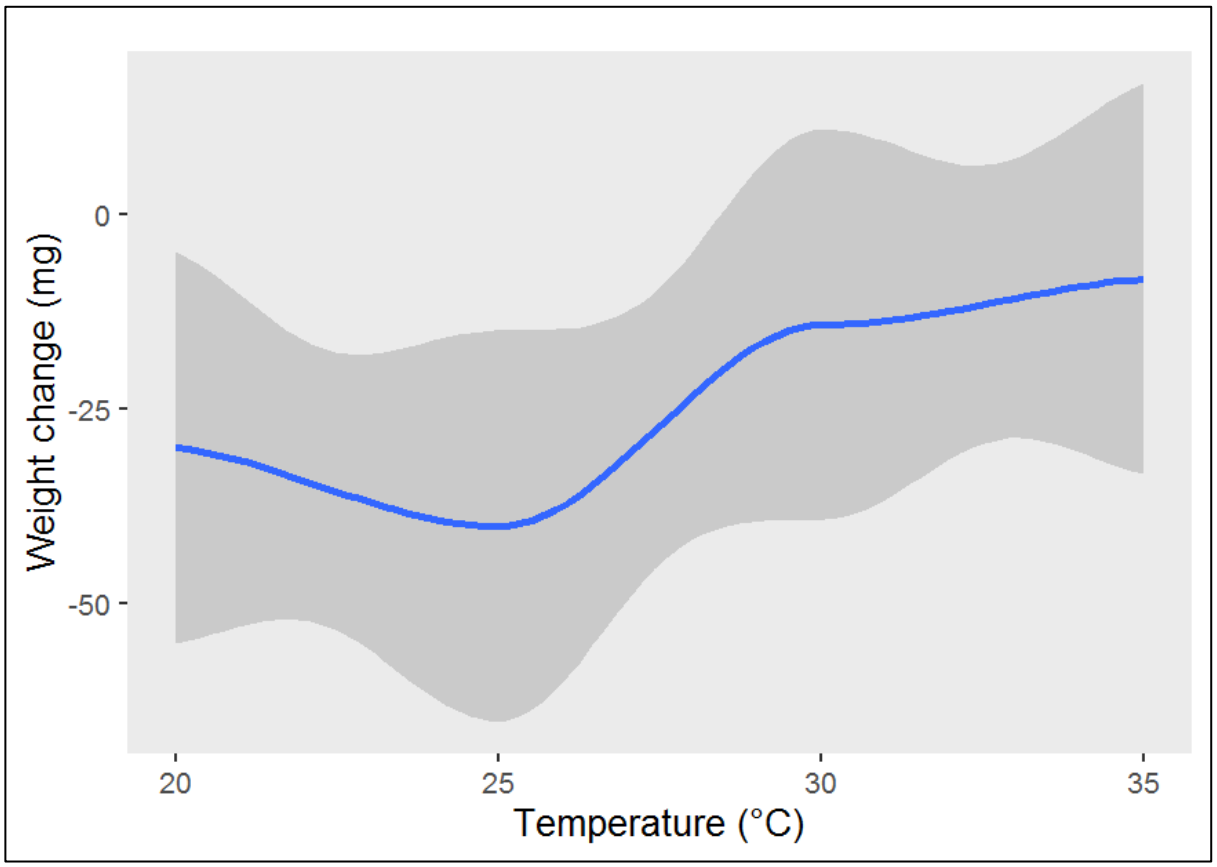

Figure A13. Weight change response associated with changing temperature at 90 parts per-thousand salinity. The blue line represents the loess smoothed mean estimate and the grey band represents the 95% confidence interval of this estimate.

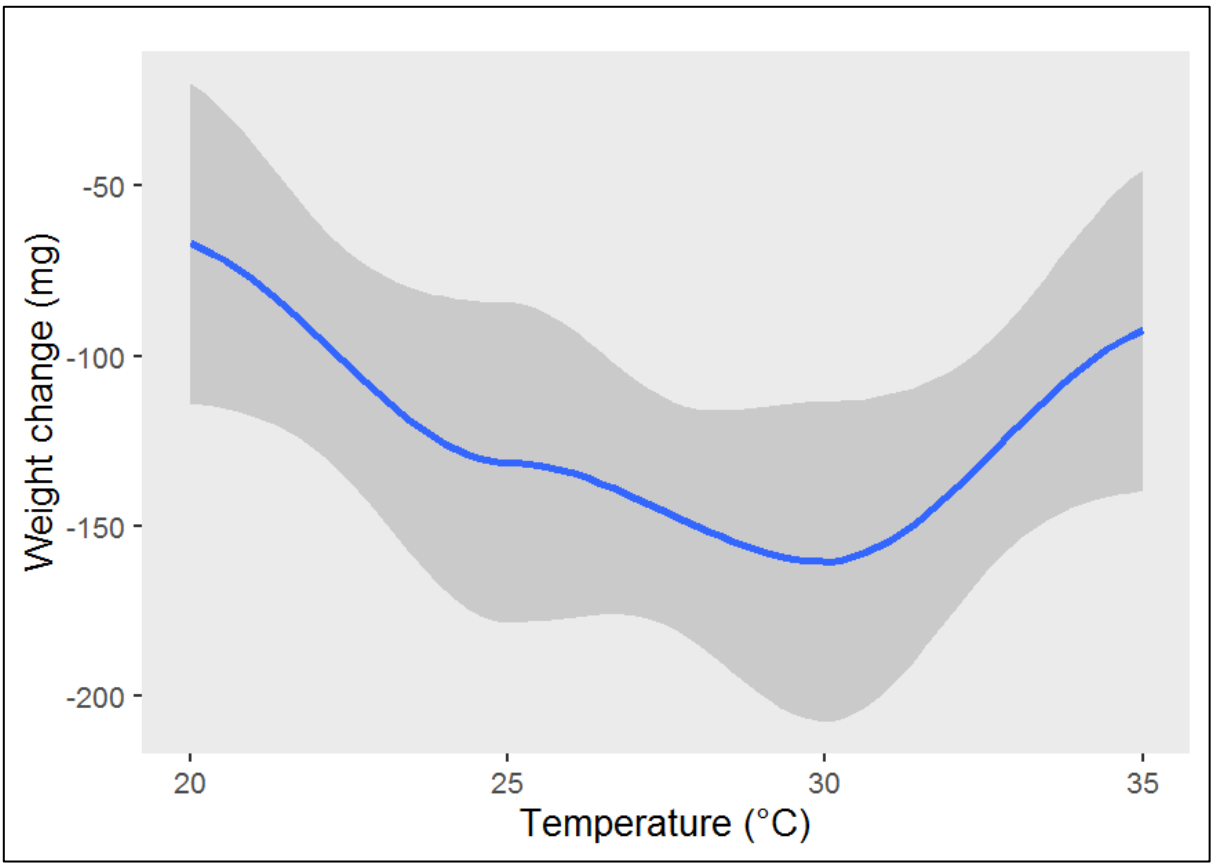

Figure A14. Weight change response associated with changing temperature at 140 parts per-thousand salinity. The blue line represents the loess smoothed mean estimate and the grey band represents the 95% confidence interval of this estimate.

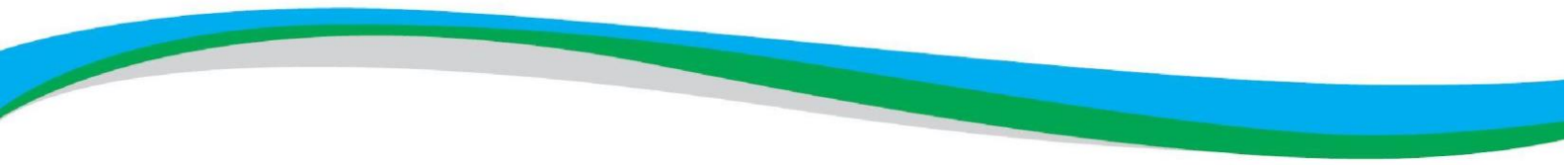

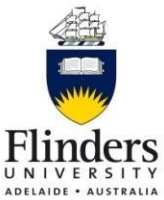

The Goyder Institute for Water Research is a partnership between the South Australian Government through the Department for Environment and Water, CSIRO, Flinders University, the University of Adelaide, the University of South Australia, and the International Centre of Excellence in Water Resource Management.